Spring 3-24-2020

Evaluation of Unmanned Aerial Systems (UAS) Imagery for Forest Regeneration Surveys

Muhammet Ali Ozderya
SUNY College of Environmental Science and Forestry, maozdery@syr.edu

Evaluation of Unmanned Aerial Systems (UAS) Imagery for Forest Regeneration Surveys

by

M Ali Ozderya

A Thesis
Submitted in Partial Fulfillment
of the Requirements for The Master of Science Degree
State University Of New York
College of Environmental Science and Forestry
Syracuse, New York
March 2020

Department of Sustainable Resources Management

Approved by:
Eddie Bevilacqua, Major Professor
Hyatt Green, Chair, Examining Committee
Chris A. Nowak, Department Chair
S. Scott Shannon, Dean, The Graduate School

ACKNOWLEDGMENT

There are number of people who have made my graduate work possible and to whom I am grateful. My major professor, Eddie Bevilacqua, for his endless patience and assistance with this thesis. Without his guidance and advice, I would not be able managed. Diane Kiernan and Jane M Read, my steering committee, for their contributions to this project. I am very grateful to professors who have servicing as my examiners, Mark Storrings and Hyatt Green. Also, I'll like to thank Mehmet Ozen who helped me at my field data collection. My friend and my family for enduring supports of all my various pursuits. Finally, the Republic of Turkey Ministry of National Education who provided me financial support that covers all my expenses during my education period.

Table of Contents

LIST OF FIGURES

LIST OF TABLES

ABSTRACT

M Ali Ozderya. Evaluation of unmanned aerial systems (UAS) imagery for forest regeneration surveys, 72 pages, 14 tables, 28 figures, 2020. Harvard – Anglia style guide used.

Accurate and reliable methods of assessing forest regeneration are necessary to improve forest inventories and assist management decisions. This research evaluates the effectiveness of high spatial resolution imagery from unmanned aerial systems (UAS) to assess abundance and structure of forest regeneration. Data were collected for 696 young Norway spruce (*Picea abies*) trees to establish field-based census. UAS digital stereo imagery was collected at three altitudes, two flight speeds and four flight azimuths, for a total of 24 separate missions. Using two orthomosaic programs, orthoimages and Digital Elevation Models (DEM) were created. Number, location and size distribution of Norway spruce trees were derived from UAS products through manual and automated processes and compared to field measurements. Manual tree detection and position estimates produced best results with 93% accuracy, while automated tree detection was only 63% accurate. Significantly strong correlations (R^2 > 55%) between UAS crown estimates and field measurements were obtained.

Keywords: Remote Sensing, Unmanned Aerial Vehicle (UAV), Tree detection, Forest Inventory

M Ali Ozderya

Candidate for the degree of Master of Science, March 2020

Eddie Bevilacqua, Ph.D.

Department of Sustainable Resources Management

State University of New York, College of Science and Forestry

Syracuse, New York

Chapter 1. INTRODUCTION

1.1. Traditional Methods of Forest Regeneration Surveys

Information from forest regeneration assessments are used to estimate current conditions of desired species, to evaluate the success of harvest operations and planting or seeding treatments, and to identify areas that may require extra silvicultural treatments. Assessment is most often done by conducting field sampling using systematically located plots throughout the forest. Even though their main purpose concerns estimating overall stocking and density, additional features on regeneration are also collected, such as diameter, height, species composition, competition, crown size, etc. (Brand, et al., 1991; Stein, 1992).

Numerous field techniques have been developed to estimate regeneration in forests, but no single method will necessarily answer all questions a forester is looking for. Generally, field methods fall into two categories: fixed area and variable area plots. Each sampling method varies in approach and data collected. Although each method has pros and cons, they can be combined or modified to satisfy more than one objective (Stein, 1992).

Fixed areas plots fall into three different approaches, namely (1) the stocked-quadrat, (2) the plot-count, and (3) the staked-point. They can assess tree size distribution, density, and are useful for monitoring changes in the same trees or plots over time (Stein, 1992).

Variable-area plots are considerably less common in regeneration surveys. With this method, plot size varies depending on the diameter or height of the regeneration being sampled. This method falls into two main approaches: (1) Distance sampling and (2) Vertical-line or vertical-point intersection sampling (Stein, 1992).

The main limitations of field sampling are the time and cost needed to derive regeneration assessments at a desired level of precision (Brand, et al., 1991).

1.2. General History of UAV Development

As a means to supplement regeneration field work, remote sensing techniques have often been incorporated in regeneration surveys. However, traditional airborne and spaceborne technologies are expensive, not always available at the desired time and provide low spatial data resolution (Siebert & Teizer, 2014). In contrast, unmanned aerial vehicle (UAVs) technologies prove to be safe, accessible, and flexible for many applications.

As with most other remote sensing systems, UAVs were initially developed by military organizations for military applications, with data collection and weapon platforms being the primary examples of usages (Watts, et al., 2012; Austin, 2011).

Subsequent to military usage, UAVs are becoming progressively appealing for many civilian purposes, including educational and commercial applications, as well as scientific data collection.

The number of papers published on UAV's, commonly referred to as drones, has increased exponentially. As Chabot (2018) reported, use of unmanned vehicle systems (UVS) for environmental monitoring and remote sensing published between 2013 and 2017 (result was obtained at 12 January 2018) increased from 544 to 1593 (Figure 1).

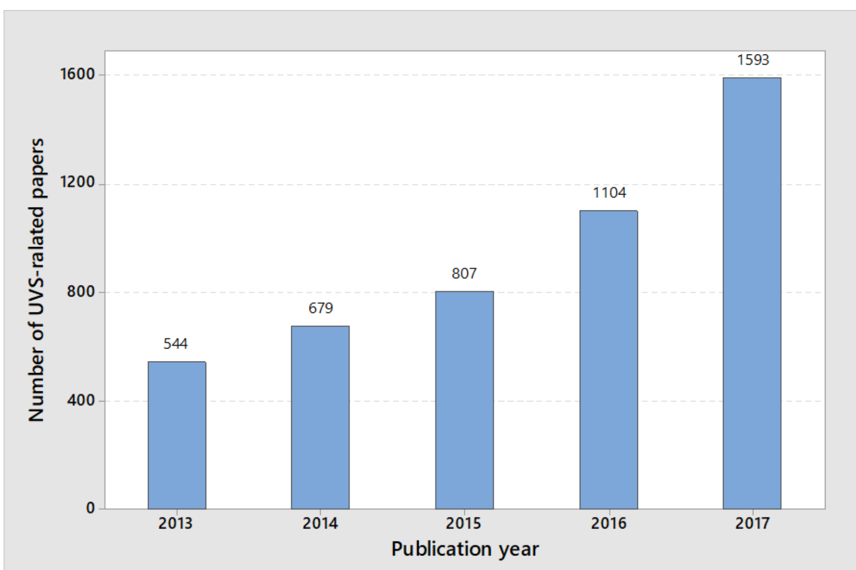

Figure 1. Amount of UVS related papers between 2013 and 2017, with search terms: "unmanned" and "drone" on the WoS (SCI-E), last updated June 12, 2018 (Chabot, 2018)

1.3. Benefits and Limitations of UAV in Environmental Research Applications

Unmanned aircraft vehicles help us to extend our potential data collection in difficult to access areas and to perform dangerous or difficult tasks safely and efficiently. Using this technology saves money and time. Current applications include forest and agriculture purposes (Saari, et al., 2011), range (Quilter & Anderson, 2000; Quilter & Anderson, 2001; Rango, et al., 2006), wildlife (Jones IV, et al., 2006), and wildlands (Göktoğan, et al., 2009) management, and emergency and disaster management (Ameri, et al., 2009).

One advantage of UAV is that they are relatively safe for pilots and crews. In hazardous conditions, such as search and rescue operations following earthquakes, volcano, or forest wildfire, using UAVs offers fast and safe data collection and monitoring of current condition. Another benefit of UAVs is their ability to fly at low altitude and gather high resolution imagery, which is essential for sampling and data collection. Moreover, they have operational flexibilities and mobilities, able to be deployed within relatively short time and less affected by cloudy conditions. Also, compared to traditional aerial remote sensing using airplanes, they require minimal runway space for landing and launching.

Another significant benefit of small UAVs is their overall lower cost. Not only they can be less expensive to buy their components and build one, but they also have low maintenance costs and low expense per flight.

Although UAVs have many advantages, limitations still exist. One is their small size and weight. During flight, any vibrations produced by maneuvers or wind causes distortion in images. Flight times and aerial coverage are limited by battery performance. Flight times are further limited by the amount of payload attached to the UAV.

1.4. Case Studies in Forest Regeneration Surveys

Aerial imagery has been used in forest applications for close to a century and are beneficial for conducting regeneration survey. Previous success of using them in forest management and inventory led them to be used in regeneration inventory (Goodbody, et al., 2017). Early work in regeneration surveys focused on large-scale photography and manual analysis (Pouliot, et al., 2002). Doing so, Kneppeck and Ahern (1987) studied airborne imagery for young forest surveys in British Colombia with great success, even though this approach was not well known at that time. Brand et al. (1991) compared Multispectral Electro-optical Imaging Scanner (MEIS) imagery with field measurement for young plantation in the Petawawa National Forestry Institute research forest. They were successful in obtaining tree counts with slightly more than 90% agreement. Forest stocking and regeneration density were studied using large-scale (1:500) photographs in Prince Albert National Park (Hall & Aldred, 1992). The study found large differences in absolute measures of density between field sampling and photo estimates and recommended such surveys should not be conducted using large-scale photography, although large-scale photos were a suitable tool for assessing stocking and survival rates. While results seem mostly positive, remote sensing methods have not been widely accepted because of either technical limitations of sensors, time consuming process of image collection and analysis, or the requirement of qualified personnel and special equipment (King, 2000).

Compared to other airborne vehicles, UAVs potentially provide quick, inexpensive, and accurate information. Because tree height and crown size are important characteristics of forest structure (Panagiotidis, et al., 2017), most of the regeneration survey using UAVs focused on estimating these attributes. Using a tree-detecting algorithm, Pouliot et al. (2002), achieved, as a best result, 91% success from 5-cm pixel imagery taken at an altitude of 196.6 m above canopy. Estimating height via point cloud processing of UAS stereo imagery has been successfully used, with strong statistical correlation ($r_s = 0.91$, $p = 0.01$) (Goodbody, et al., 2018). Panagiotidis et al. (2017) used DJI S800 carrying a RGB camera with 5 cm resolution to estimate tree crown and height and achieved acceptable results, with RMSE% in range 11.4-12.6% and 14.3-18.6%, respectively.

1.5. Norway Spruce (Picea abies)

Norway Spruce is very widely spread in Northern and Central Europe (Hosley, 1936). The tree can find at an altitude of around 3000 m from sea level (Reynisson, 2011).

Trees can achieve heights of around 40 to 50 m and diameters up to 100 to 150 cm in its natural range. They have a conical crown. The branchlets are small and strong. The leaves vary from 1 to 2.5 cm in length and are medium to dark green (Anon., 2020). They can live up to 500 years (Woolsey & Greeley, 1920).

New York State Wood Products Development Council go into partnership with Northeastern Lumber Manufacturers Association to provide funding needed for Norway spruce lumber testing. This led to Norway spruce to the first U.S.-grown softwood species to be accepted for use in the construction since research started in the 1920s (Wood Products Development Council, 2017). New York state alone has adequate Norway Spruce to harvest at its current rate for 90 years (LBM Journal, 2017).

1.6. UAV Research Gaps

Studies on Norway spruce regeneration have been performed often in Europe (Diaci, et al., 2000; Baier, et al., 2007; Juntunen & Neuvonen, 2006a; Juntunen & Neuvonen, 2006b; Szydlarski & Modrzyński, 2015; Meyer, et al., 2017; Dănescua, et al., 2018). Compared to Europe, much less research on regeneration has been conducted in New York. Although there is abundant research on regeneration surveys involving remote sensing techniques in the last decades, Norway spruce is rarely a species that has been studied. Larsen (1997), Brandtberg and Walter (1998a; 1998b; 1999), and Erikson (2003) studied tree-crown detection algorithms by using high resolution imagery on mature Norway spruce stands. Panagiotidis et al. (2017) estimated tree height and crown diameter of tall, widely spaced Norway spruce trees from high-resolution UAV imagery and concluded methods were accepted for detecting heights and crown diameter. Heinzel and Ginzler (2019) and Puliti, et al. (2019) used unmanned aerial vehicle to evaluate regeneration height and density in young boreal forest stands and concluded the use of UAVs for inventorying regeneration can be beneficial compared to traditional field assessments.

Remote sensing practices that enhance Norway spruce regeneration surveys have not been studied in Central New York. Most studies in Europe focused their research on natural regenerated stands, although artificial regeneration was been the primary regeneration method used in Central New York. This paper will provide a case study on using UAVs to estimate density and size distribution in a young planted Norway spruce stand.

Chapter 2. GOALS AND OBJECTIVES

The aim of this project is to evaluate whether current regeneration survey methodologies can be improved using Unmanned Aerial System (UAS) by reducing time and expenses spent while improving efficiency and productivity. The overall goal of the report is to determine if we could use UAS to estimate difficult to measure features of the regeneration.

Specific objectives are:

1. Establish a field-based census of Norway spruce to use as ground-truth measurements. Field measurements will be collected on every tree, including diameter-at-breast, ground-level diameter, crown width, tree height and mapping individual tree coordinates using trilateration.

2. Perform UAV missions over the study area and collect raw and jpeg images at 100, 150, and 200 ft (30, 45, and 60 m, respectively).

3. Process collected imagery and create orthoimage and 3D digital surface model.

4. Identify individual trees, tree locations, crown area and crown volume using orthoimage and 3D digital surface model.

5. Compare calculated UAV derived tree and crown data with field measurement in order to evaluate precision.

Chapter 3. METHODS

3.1. Study Area

The research site, Norway spruce plantation, is located in the Svend O. Heiberg Memorial Forest which lies across both Onondaga and Cortland Counties within the towns of Tully, Fabius, Pompey, and Truxton in New York State (Figure 3) (ESF; Briggs, 2001). The study area is a young 30-year-old planted Norway spruce forest situated on the northern limit of the forest property at an elevation of 520 m.

The climate at the study area has average annual maximum and minimum temperatures of 11.2°C and 1.9°C, respectively. The annual precipitation is 1181 mm, with most of it falling in May through September and the least in January through February. Average snow fall is 3124 mm and the snow cover reaches 10.1 cm (Western Regional Climate Center, 2007).

There are three discrete young Norway spruce groups located in the third management compartment: 0.4, 0.5 and 1.2 ha in size. We chose to study the 0.5-hectare stand, located on the southeast portion of the compartment. The study area is a rectangular shape which has a length of 160 m and a width of 35 m. Individual trees have crowns and branches extending close to the ground or grown into clusters with significant crown overlap and complete crown closure.

Figure 2. Visual representation of a small portion of the study area

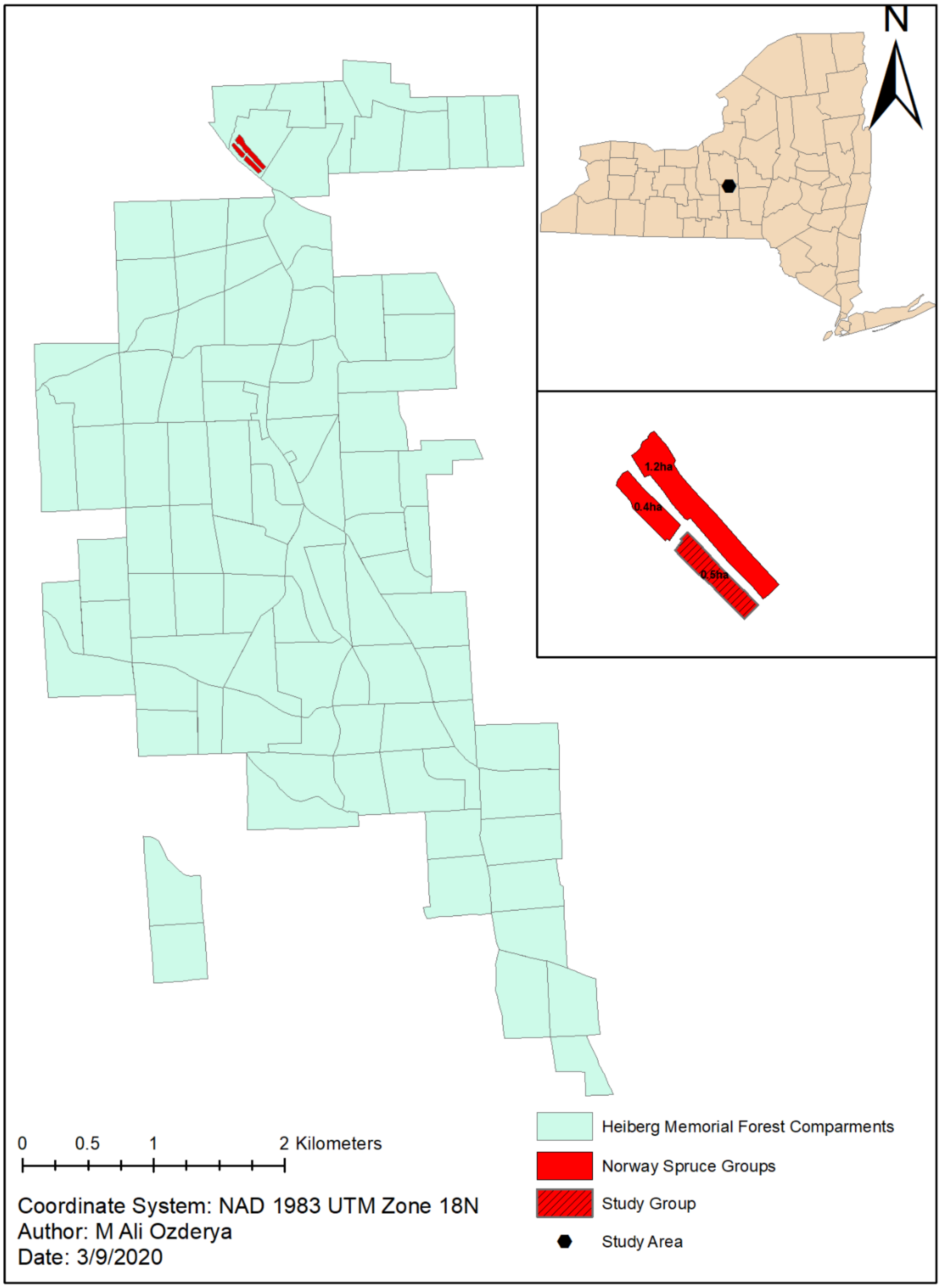

Figure 3. Location of Study Area

3.2. Ground Data Collections

Regeneration data was collected in the autumn of 2018 and took about 25 days. For validation of tracking data, starting from east side of the plot, trees were tagged and enumerated. Diameter-at-breast height (DBH, 1.3 m or 4.5 ft above the ground) and diameter-at-ground-level (DGL) were measured to the nearest 0.1 cm with a diameter tape. Crown width was measured to the nearest 1 cm in north-south, and east-west directions at the crown base, using a tape measure and arithmetic average taken to single value. Tree heights were measured to the highest live point of the crown, to the nearest 3 cm.

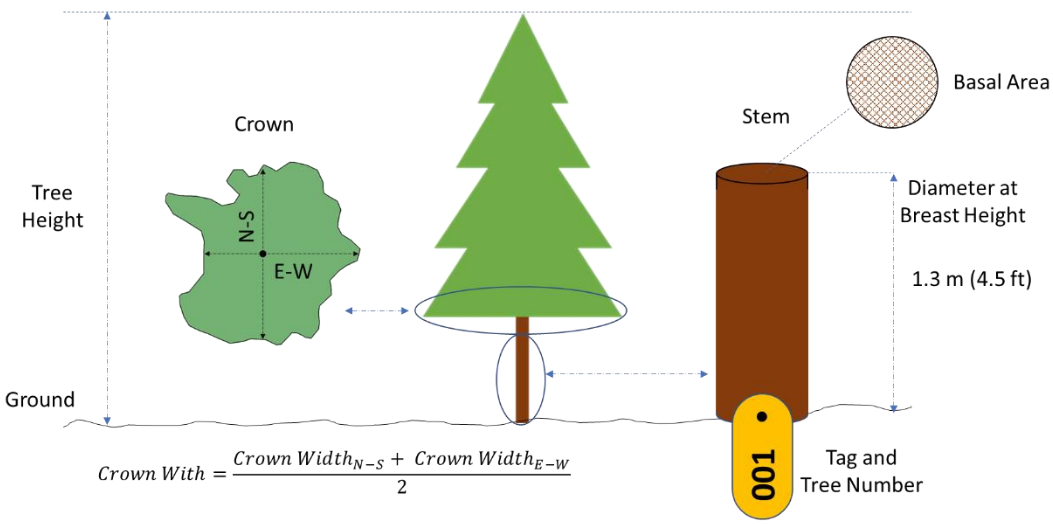

$$Crown\ With = \frac{Crown\ Width_{N-S} + Crown\ Width_{E-W}}{2}$$

Figure 4. Some tree attributes that collected at field

3.2.1. Mapping Trees Using Distance Measurements and INTERPNT

The next step of field study was to map the location of trees using INTERPNT, a computer program developed at Harvard University in 1990 (Boose, et al., 1998). The computer program applies the principles of trilateration to calculate the coordinates of an unknown position in a two-dimensional space by measuring distances from three known positions (Figure 5). Three reference points (benchmarks) were set up and cartesian coordinates were obtained by a tripod-mounted Trimble Geo XH 3000 GPS Unit. As mentioned in the ground data collection section, individual trees were already tagged with plastic or metal tags and their DBH measured. To calculate coordinates of each target tree, three distances measured to the nearest 0.1 cm using a Leica DISTO laser distance measurer were obtained from either benchmarks or previously located trees (Figure 5, Table 1).

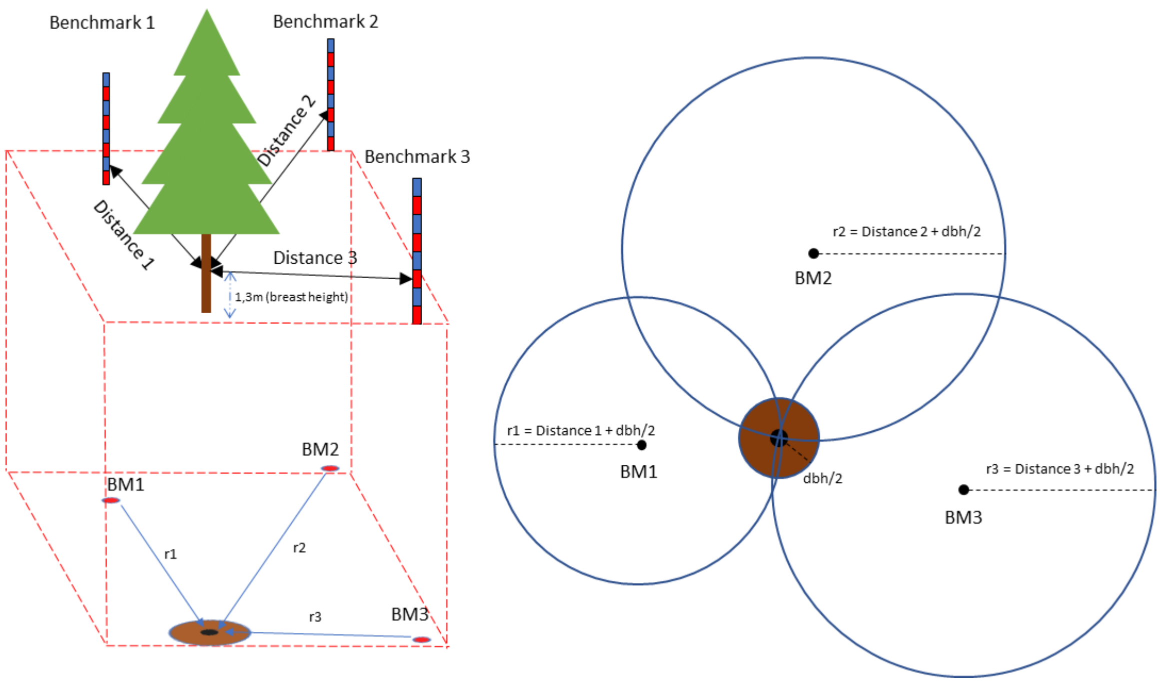

Figure 5. Illustration of trilateration method

Table 1. Example of first 5 tree distance measurement

Tree	dB	target1	dist1	target2	dist2	target3	dist3	x	y	diff1	diff2	diff3
BM1	2.5							411138	4737164			
BM2	2.5							411141	4737160			
BM3	2.5							411137	4737157			
1	11.9	BM1	3.775	BM2	4.651	BM3	3.754	411137	4737161	0.06	-0.11	0.06
2	14.8	BM1	6.089	BM2	6.598	BM3	3.545	411135	4737159	-0.02	0.01	-0.02
3	11.6	BM1	3.590	BM2	6.717	BM3	6.096	411135	4737162	0.06	-0.04	0.06
4	7.5	3	2.526	1	3.397	2	2.123	411133	4737160	-0.08	0.05	-0.07
5	6.2	3	2.275	2	5.328	4	3.678	411133	4737164	0.04	-0.02	0.03
The data collected and recorded by user								Coordinates and individual distance errors calculated by computer program				

3.3. UAV Data Collection

For this research we used a 3DR Solo quadcopter mounted beneath with two MAPIR Survey 2 cameras, a near infrared (IR) and a visible band red-green-blue (RBG). Missions for this UAS with the above payload would last for up to 20 minutes.

Three UAV mission parameters were modified for each flight, as presented in Figure 6 and described below, for a total of 2x4x3 = 24 separate flights:

1. 2 flight speeds (5 mph and 8 mph);
2. 4 flight azimuths (0°, 45°, 90°, and 135°); and
3. 3 altitudes above ground level (30, 45, and 60 m [100, 150, and 200 ft, respectively]).

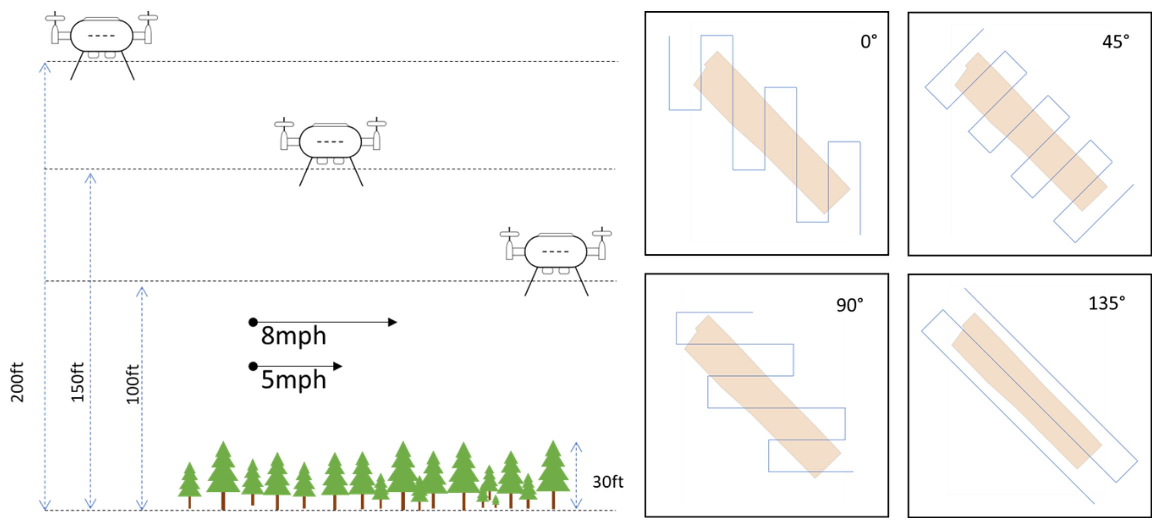

Figure 6. Flight altitudes and flight angle (all distances are drawn to scale).

The Tower software (DroidPlanner, 2016) was used for flight planning. This software allows user input for all flight parameters and then operates the flight automatically. All the missions were set up to acquire stereo imagery with a front overlap of 85% and a side overlap of 80%. Geosetter (Schmidt, 2019) was used to geotag images while MAPIR Camera Control Kernel program was used to process raw images to convert to either tiff or jpg images.

3.4. Derived Products from Stereo Imagery

DroneDeploy (DroneDeploy, 2019) and Agisoft Metashape Professional (Agisoft, 2019) were used to create orthoimages, generate point cloud layers and produce a digital elevation model of canopy surface for each mission's set of stereo imagery.

3.5. Manual and Automated Tree Detection

3.5.1. Manual Tree Identification and Measurement

Manual individual tree identification was conducted using only the orthoimage derived from 5 mph RGB imagery. The orthoimages from all IR and 8 mph RGB imagery were dropped for manual identification because human eyes could hardly distinguish individual trees from their surroundings due to similar pixel values in IR while quality of orthoimage from 8 mph was very low and had lots of distortion.

All usable orthoimages were added to ArcMap, and the Georeferencing Toolbar used reference images to readily available base maps to minimize distortions and increase accuracy. Between 10 and 12 control points were used until an acceptable (average 2.2 cm) Root Mean Squared Error (RMSE) was obtained. The Circle Construction Tool from Editor Toolbar was used to manually delineate tree crowns (Figure 7). At the conclusion of this step, all individual trees crown areas and locations were visually and attributively acquired.

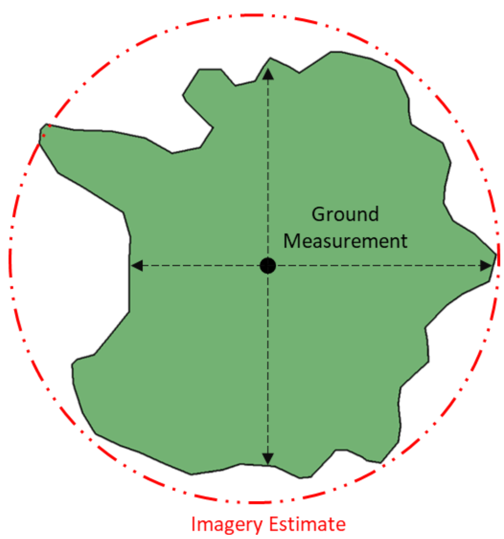

Figure 7. Example of manually created tree crown by using Circle Construction Tool

3.5.2. Automated Tree Detection

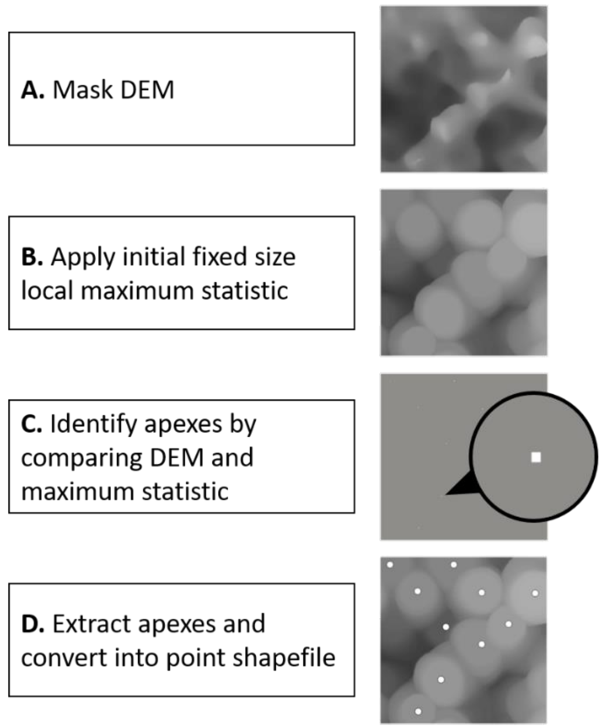

Figure 8. Overview of automated tree detection process.

Automated individual tree detection was conducted using the 3D digital elevation model (DEM) derived from the stereo imagery. A cartographic model was developed using local maxima principles. The process of tree detection consists of the four steps indicated in Figure 8. In the first step (A), DEMs are masked in order to eliminate detection of trees outside of study area. This step also helps to reduce noise by preventing mistaken detection of local maximum in vegetation.

In the second step (B), a local maxima statistic was applied from the DEM. Among the several neighborhood settings tested, including different shapes and units, the best results were achieved using a circle with a 1-m radius for DroneDeploy and 1.5-m radius for Agisoft.

In the third step (C), the raster calculator is executed by the Boolean logic expression that returns 1, or “true” when the local maxima filter and the DEM are matched, and if not, 0, or “false”. In order to filter apexes, the Reclassify Tool was used to convert value 0 to NoData. In the last step (D), the cells representing tree apexes were converted into point shapefile.

3.6. Assessment of Individual Tree Detection and Crown Delineation

3.6.1. Individual Tree Detection Accuracy

The accuracy of manual and automated individual tree detection (image-trees) was evaluated by comparing and matching their locations to field-based measurements (i.e., field-tree). Three types of tree detection parameters were evaluated: true positive (TP, correctly detected), false negative (FN, could not detected) and false positive (FP, does not exist but is detected).

For manually detected trees, each image-detected tree was deemed to be a TP (have a matching field-tree) when a field-tree's crown significantly overlapped the image-tree's crown, otherwise the image-tree was considered a FP. Field-trees without a paired image-tree were considered an FN.

For automated identified trees, image-tree apexes closest to and within field-tree crowns were assigned as TP. Image-tree apexes not overlapping field-tree crowns were FP, while field-trees without a paired image-tree were considered an FN. In order to evaluate the overall accuracy of the detection, omission and commission errors and accuracy index were calculated using the following equations:

Commission Error refers to the percentage of trees incorrectly included in the population, computed as the ratio of FP to total number of detected trees. Omission Error refers to the percentage of trees that were undetected from the population, computed as the ratio of FN to total number of field trees. Accuracy Index refers the percentage of detected trees against all errors.

$$Commission\ \ Error\ (\%)\ = \frac{FP}{FP+TP}\ x\ 100 \qquad (1)$$

$$Omission\ Error\ (\%) = \frac{FN}{FN+TP}\ x\ 100 \qquad (2)$$

$$Accuracy\ Index\ (\%) = \frac{n\ -\ (O\ +\ C)}{n}\ x\ 100 \qquad (3)$$

where *O* and *C* are the number of omission and commission errors, and *n* is the total number of field trees.

3.6.2. Positional Accuracy

Positional accuracy of a tree is calculated as the Euclidean distance between field- and image-tree position. After matching all true-positive (TP) image-trees from manual and automated tree detection procedures, positional accuracy of image-tree locations was evaluated using mean and RMSE distance between field- and image-tree coordinates.

3.6.3. Delineation Accuracy

After matching all true-positive (TP) image-trees from manual and automated tree detection procedures, assessment of image-based estimates of crown area were evaluated using Root Mean Square Error (RMSE) and Root Mean Square Error as a percentage of the mean true value.

$$RMSE\ (m)\ = \sqrt{\frac{\sum(\hat{Y}_i - Y_i)^2}{n}} \tag{4}$$

$$RMSE\ (\%)\ = \frac{100}{\bar{Y}}\ x\ \sqrt{\frac{\sum(\hat{Y}_i - Y_i)^2}{n}} \tag{5}$$

where $\hat{Y}_i$ is predicted value driven from imagery, Y_i is ground measurement, *n* is number of observations, and $\bar{Y}$ is mean value of ground measurement.

3.6.4. Assessment of Tree-Level Predictions

After matching all true-positive (TP) from image-trees, the assessment of image-tree estimates of crown area was evaluated using fit statistics, i.e., coefficient of determination (R^2) and Root Mean Squared Error (RMSE), from linear regression analysis. All regression equations using image-based crown area estimates as the independent variable, and field-based tree measurements (i.e., tree basal area and crown area) as dependent variables.

Chapter 4. RESULTS

4.1. Field Data

A total of 696 young Norway spruce were identified and mapped, and measurements of their size was gathered. The statistics are summarized in detail at Table 2. Distribution of all variables is not symmetric, each skewed to the left (Figure 9).

Table 2. Summary statistics of diameter-at-breast height (DBH), diameter-at-ground level (DGL), tree height, and crown width

	Mean	Median	Std.Dev.	Min	Max
DBH (cm)	7.52	8.00	3.37	0.00	16.30
DGL (cm)	11.15	11.60	4.43	0.90	21.80
Height (m)	5.21	5.45	1.73	0.46	9.32
Crown Width (m)	2.63	2.71	0.85	0.29	5.52

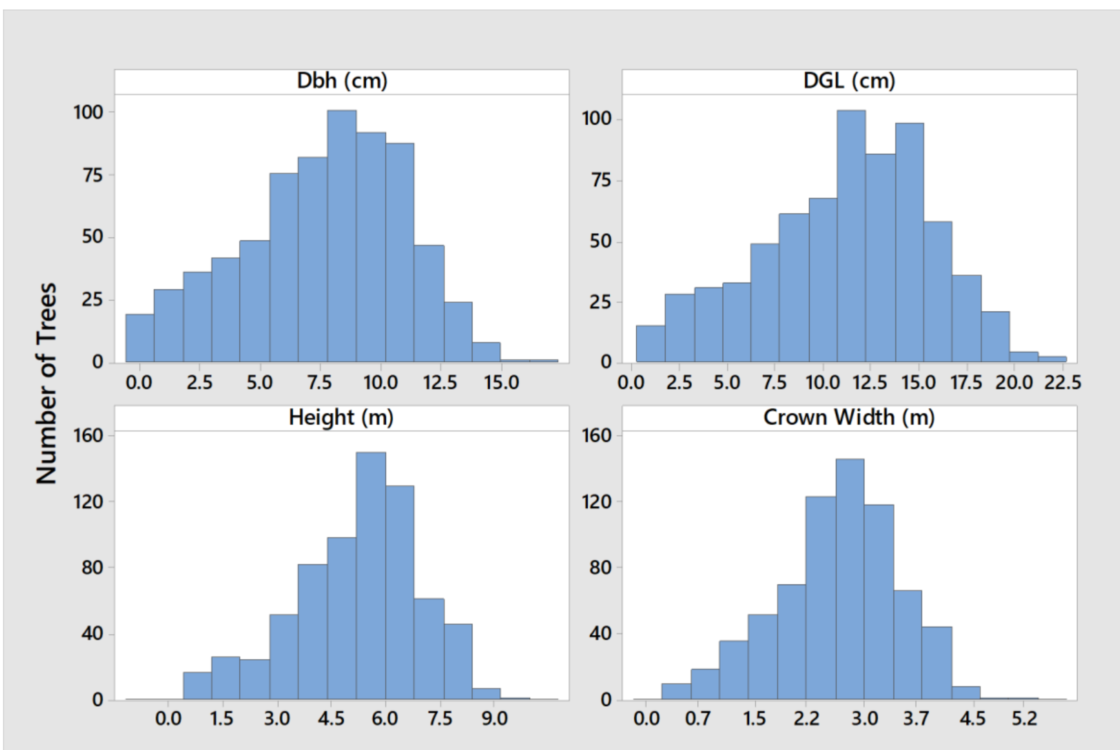

Figure 9. Frequency distributions of measured diameter-at-breast height (DBH), diameter-at-ground level (DGL), tree height, and crown width

4.2. Crown Overlap

After creating a stem map derived from trilateration method, crown areas of individual trees were created using Buffer and Elliptical tools in ArcMap. There was no distinguishable difference between the two approaches due to symmetrical characteristic of crowns. Over 230 trees (approx. 33%) have crowns that more than 25 percent overlap with neighboring trees' crowns. The remaining trees had crowns that either did not overlap at all or only up to 25 percent overlap with other trees.

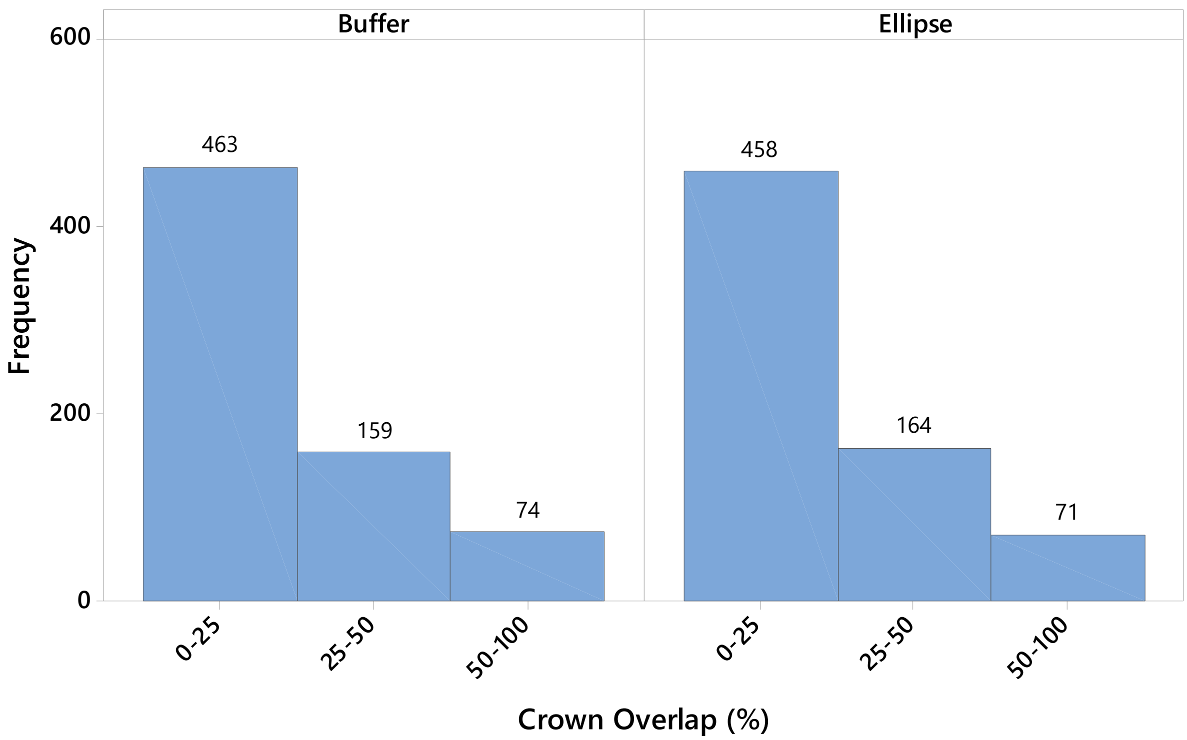

Figure 10. Frequency distributions of crown overlap

4.3. Missions

As expected, increasing the flight altitude generally decreased the flight duration with fewer images taken. However, increasing the flight speed surprisingly decreased front image overlap. Decreased front image overlap is unexpected because we programmed the drone for specific overlap. The exception for this can be seen in Table 3 and Table 4 with an altitude 100 m and 90° and 135° flight azimuths. Because each mission was generated independently, the coverage of each mission varied, sometimes resulting in more photos to be produced at a faster mission than the slowest mission counterpart. Within the same mission, two different cameras (IR and RGB) were initiated together, but after a certain period of time, became unsynchronized due to small fluctuations in the writing speed of saving picture to a microSD card. Thus, this issue made the IR and RGB pictures incompatible to combine with each other in any subsequent processing steps. Some pictures were discarded because they covered very little of the study area (Figure 11) and had a negative effect on the orthoimage quality. In total, 3674 images (1860 RGB and 1814 IR) were taken and 660 images (349 RGB and 311 IR) were discarded.

Figure 11. An example of a discarded picture from the mission at 150 ft altitude with 0-degree flight angle

Table 3. Summary of UAS missions using the visible RGB camera

Altitude (ft)	Hatch Angle	Speed (mph)	Date flown	Time of flight	Duration (min)	Number of images		Pixel Resolution* (mm)	Storage (GB)
						Images acquired	Images used		
100	0	5	6/27/2019	2:07 PM	12	115	78	10.3	3.92
		8	6/23/2019	11:06 AM	7	82	66	10.3	2.80
	45	5	6/27/2019	2:32 PM	11	111	84	10.3	3.79
		8	6/23/2019	11:23 AM	7	90	78	10.3	3.06
	90	5	6/23/2019	10:15 AM	11	109	85	10.3	3.71
		8	6/23/2019	11:47 AM	10	123	65	10.3	4.19
	135	5	6/23/2019	10:41 AM	9	80	80	10.3	2.72
		8	6/23/2019	12:16 PM	7	84	57	10.3	2.86
150	0	5	6/22/2019	10:46 AM	11	128	84	15.4	4.36
		8	6/27/2019	1:40 PM	7	67	43	15.4	2.29
	45	5	6/22/2019	11:21 AM	10	119	89	15.4	4.06
		8	6/23/2019	12:50 PM	6	50	47	15.4	1.71
	90	5	9/8/2019	12:29 AM	8	93	86	15.4	3.17
		8	6/23/2019	1:12 PM	6	51	42	15.4	1.74
	135	5	9/8/2019	12:56 AM	7	79	77	15.4	2.69
		8	6/23/2019	1:34 PM	4	51	47	15.4	1.74
200	0	5	6/27/2019	3:15 PM	8	63	60	20.6	2.15
		8	6/23/2019	1:51 PM	4	46	44	20.6	1.57
	45	5	6/27/2019	3:40 PM	8	63	63	20.6	2.14
		8	6/23/2019	2:05 PM	5	43	43	20.6	1.47
	90	5	6/27/2019	3:58 PM	7	59	59	20.6	2.01
		8	9/8/2019	11:52 AM	5	54	40	20.6	1.60
	135	5	6/27/2019	3.28 PM	8	60	48	20.6	2.05
		8	6/23/2019	2.23 PM	5	47	39	20.6	1.60

*The pixel resolution was derived from the MAPIR Camera Flight Calculator (MAPIR CAMERA, 2020).

Table 4. Summary of UAS missions using the near-IR camera

Altitude (ft)	Hatch Angle	Speed (mph)	Date flown	Time of flight	Duration (min)	Number of images: Images acquired	Number of images: Images used	Pixel Resolution* (mm)	Storage (GB)
100	0	5	6/27/2019	2:07 PM	12	114	73	10.3	3.87
		8	6/23/2019	11:05 AM	7	76	59	10.3	2.58
	45	5	6/27/2019	2:30 PM	11	118	95	10.3	4.00
		8	6/23/2019	11:20 AM	7	89	72	10.3	3.03
	90	5	6/23/2019	10:15 AM	11	116	87	10.3	3.96
		8	6/23/2019	11:47 AM	10	126	75	10.3	4.29
	135	5	6/23/2019	10:40 AM	9	84	84	10.3	2.86
		8	6/23/2019	12:15 PM	7	88	61	10.3	2.99
150	0	5	6/22/2019	10:45 AM	11	137	80	15.4	4.66
		8	6/27/2019	1:40 PM	7	64	51	15.4	2.16
	45	5	6/22/2019	11:10 AM	10	102	76	15.4	3.46
		8	6/23/2019	12:50 PM	6	45	41	15.4	1.52
	90	5	9/8/2019	12:29 AM	8	93	91	15.4	3.17
		8	6/23/2019	1:10 PM	6	49	45	15.4	1.66
	135	5	9/8/2019	12:55 AM	7	77	75	15.4	2.61
		8	6/23/2019	1:30 PM	4	49	49	15.4	1.66
200	0	5	6/27/2019	3:10 PM	8	67	63	20.6	2.26
		8	6/23/2019	1:50 PM	4	34	33	20.6	1.15
	45	5	6/27/2019	3:40 PM	8	59	59	20.6	1.99
		8	6/23/2019	2:05 PM	5	47	47	20.6	1.59
	90	5	6/27/2019	3:58 PM	7	61	57	20.6	2.06
		8	9/8/2019	11:54 AM	5	52	39	20.6	1.78
	135	5	6/27/2019	3.28 PM	8	72	59	20.6	2.44
		8	6/23/2019	2.22 PM	5	47	42	20.6	1.58

*The pixel resolution was derived from the MAPIR Camera Flight Calculator (MAPIR CAMERA, 2020).

4.4. Orthoimage Creation

Creation of orthoimages was more successful using DroneDeploy, as compared to Agisoft. For nearly half of the missions, Agisoft was unable to generate a useful orthoimage. In contrast, DroneDeploy failed to produce an orthoimage only twice.

Table 5. Summary of orthoimage productivity

Flight Altitude	Number of flights*	Number of successful orthoimages created			
		Agisoft		DroneDeploy	
		5mph	8mph	5mph	8mph
100 ft	4	2	2	3	3
150 ft	4	2	2	4	4
200 ft	4	4	2	4	4

* Hatch angle and flight speed combined

4.5. Orthoimage Visual quality comparison between DroneDeploy and Agisoft

The spatial resolution of orthoimages achieved by the both Agisoft and DroneDeploy were very high, with DroneDeploy having slightly smaller resolution. Altitude and speed had an impact on visual quality, with imagery obtained at higher altitudes producing reduced quality orthoimages, while increase in speed creates additional visual quality problems.

Although the resolution of orthoimages was very high, there were some difficulties in using the resulting images. First, there are data gaps in some orthoimages, which creates up to 20 voids of different sizes and shapes (Figure 12 A). Second, "blotches" that drop the quality of image and make individual tree identification difficult (Figure 12 B). With nature of IR camera having only has one spectral band, reducing contrast around crown edges, limiting one's ability to identify individual trees (Figure 12 C).

Overall, having fewer blotches and gaps, DroneDeploy produces clearer images, sharper crown edges, and individual trees with more details as compared to images produced using Agisoft.

Table 6. Summary of orthoimage resolution

Flight Altitude	Speed (mph)	Average Orthoimage resolution (cm/pix)			
		Agisoft		DroneDeploy	
		RGB	IR	RGB	IR
100 ft	5	1.13	1.25	1.09	1.07
	8	1.08	1.13	1.04	1.02
150 ft	5	1.60	1.68	1.30	1.27
	8	2.53	2.16	1.57	1.55
200 ft	5	2.29	2.04	2.13	2.06
	8	2.60	2.20	2.09	2.05

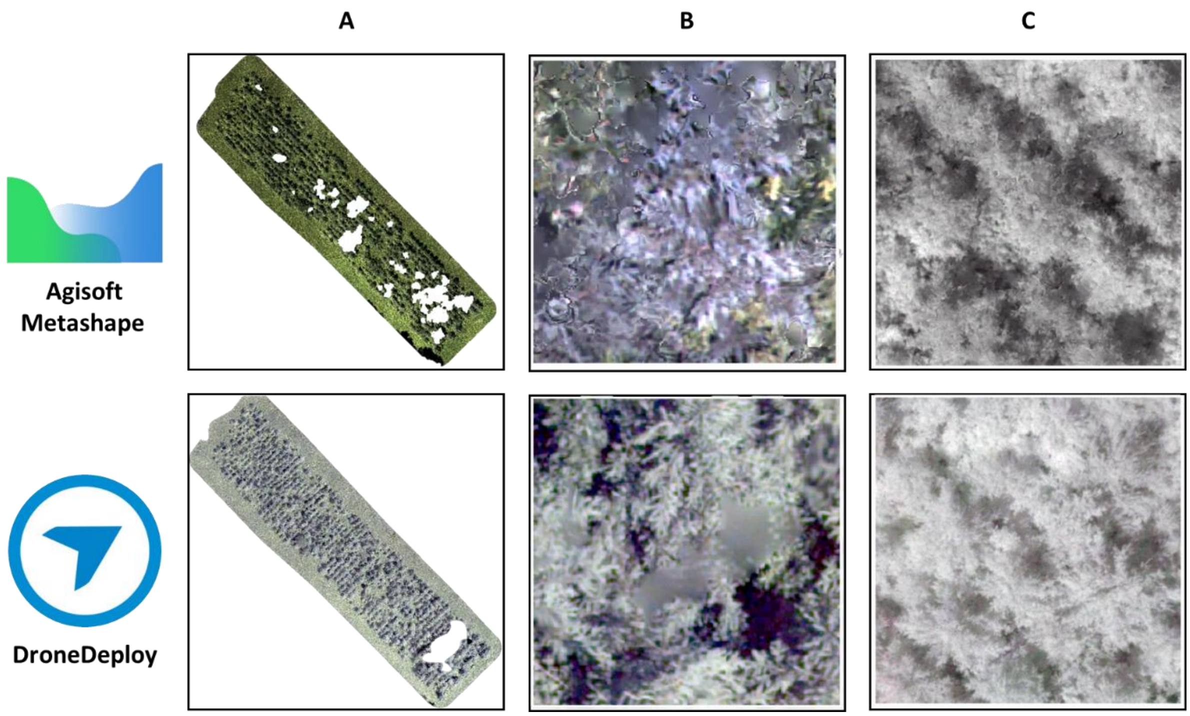

Figure 12. Examples of some distortion at orthoimeges A) Gaps B) Blotches C) lack of contrast around crown edges

4.6. Individual Tree Detection

4.6.1. Manual Tree Detection

Overall accuracy from manual detection of treetops using orthoimages generated by both image analysis computer programs—i.e., DroneDeploy and Agisoft—was very high, accuracy indices around 90%. Manual tree detection from DroneDeploy orthoimages has lower amounts of omission and commission error as compared to tree detection from Agisoft orthoimages (Table 7). Missed trees on the DroneDeploy orthoimages are mostly from the very small diameter class of 0-2 cm (Figure 13), while Agisoft produced orthoimages that resulted in more missed trees from larger DBH classes (Figure 14). There were no discernable differences in the frequency distribution of missed trees by DBH class among UAV missions (Figure 13). However, the orthoimages created from missions flown at 135^{o} azimuth (i.e., parallel to the planting row orientation) generally resulted in the smallest proportion of missed trees (Table 7).

Errors of commission—i.e., detecting a tree that isn't there—were relatively rare compared to errors of omission for all orthoimages.

Table 7. Summary of manual tree detection accuracy

Computer Program	Altitude (ft)	Hatch Angle	Detected Tree	Omission (%)	Commission (%)	Accuracy Index (%)
DroneDeploy	100	0	613	11.93	0.65	87.64
		45	N/A	N/A	N/A	N/A
		90	642	7.76	0.62	91.67
		135	650	6.61	0.31	93.10
	150	0	631	9.34	0.79	89.94
		45	630	9.48	0.63	89.94
		90	638	8.33	0.62	91.09
		135	650	6.61	0.76	92.67
	200	0	646	7.18	1.52	91.38
		45	633	9.05	1.25	89.80
		90	629	9.63	1.10	89.37
		135	643	7.61	0.62	91.81
Agisoft	100	0	N/A	N/A	N/A	N/A
		45	590	15.23	0.67	84.20
		90	N/A	N/A	N/A	N/A
		135	640	8.05	1.99	90.09
	150	0	638	8.33	2.00	89.80
		45	N/A	N/A	N/A	N/A
		90	N/A	N/A	N/A	N/A
		135	614	11.78	1.13	87.21
	200	0	572	17.82	1.55	80.89
		45	606	12.93	1.46	85.78
		90	614	11.78	1.44	86.93
		135	613	11.93	3.77	84.63

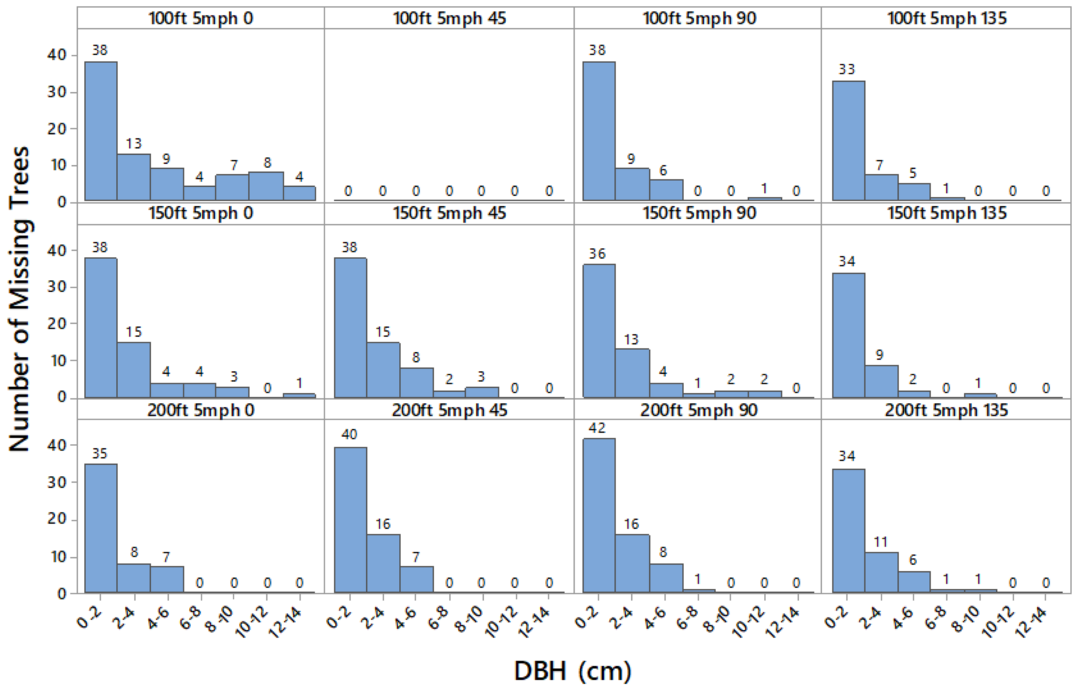

Figure 13. Frequency distribution of missing trees from manual tree detection by DBH class using orthoimages created by DroneDeploy

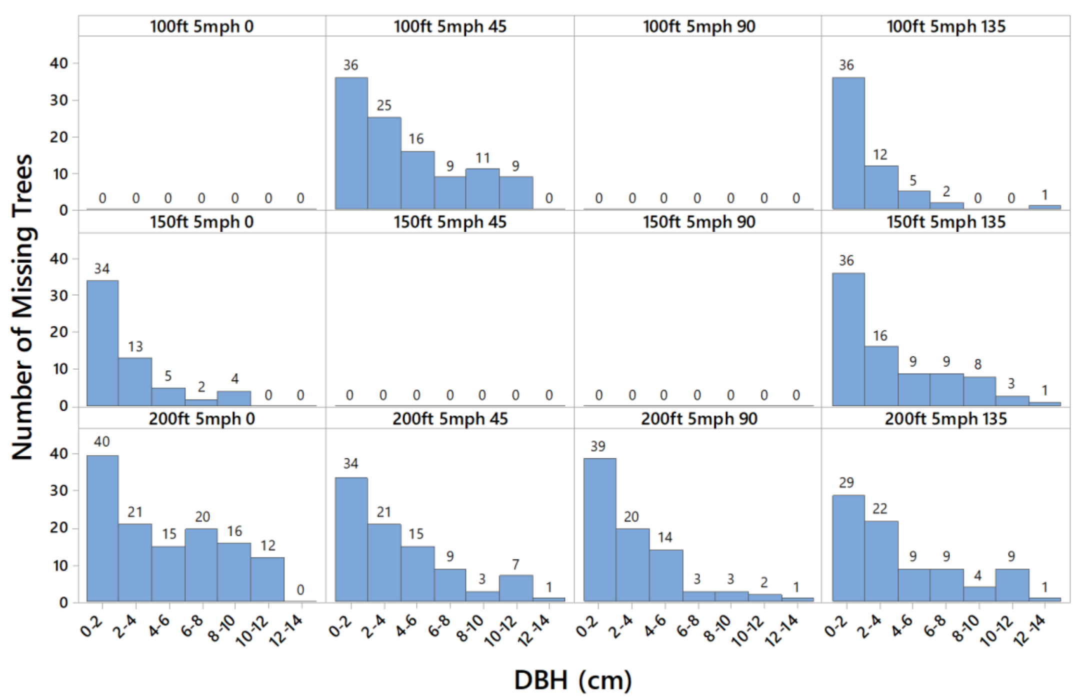

Figure 14. Frequency distribution of missing trees from manual tree detection by DBH class using orthoimages created by Agisoft

4.6.2. Automated Tree Detection

Compared to manual tree detection, automated tree detection accuracy from 3D canopy surfaces was very low, with accuracy indices averaging at 50% for DroneDeploy and 38% for Agisoft (Table 8). This was the result of increased errors of both omission and commission. Canopy surfaces derived from 200 ft missions produced fewer errors of commission compared to 100 and 150 ft missions. Unlike manual tree detection, there was no pattern in detection accuracy among the missions with different azimuths.

Table 8. Summary of automated tree detection accuracy

Computer Program	Altitude (ft)	Hatch Angle	Detected Tree	Omission (%)	Commission (%)	Accuracy Index (%)
DroneDeploy	100	0	307	55.89	23.63	30.46
		45	N/A	N/A	N/A	N/A
		90	463	33.48	12.14	57.33
		135	417	40.09	12.94	51.01
	150	0	448	35.63	10.58	56.75
		45	421	39.51	10.23	53.59
		90	511	26.58	12.20	63.22
		135	495	28.88	14.51	59.05
	200	0	418	39.94	5.64	56.47
		45	394	43.39	6.19	52.87
		90	409	41.24	7.26	54.17
		135	385	44.68	7.89	50.57
Agisoft	100	0	N/A	N/A	N/A	N/A
		45	334	52.01	30.27	27.16
		90	N/A	N/A	N/A	N/A
		135	375	46.12	18.12	41.95
	150	0	380	45.40	24.30	37.07
		45	N/A	N/A	N/A	N/A
		90	N/A	N/A	N/A	N/A
		135	365	47.56	24.12	35.78
	200	0	371	46.70	19.70	40.23
		45	385	44.68	18.78	42.53
		90	379	45.55	17.97	42.53
		135	368	47.13	21.54	38.36

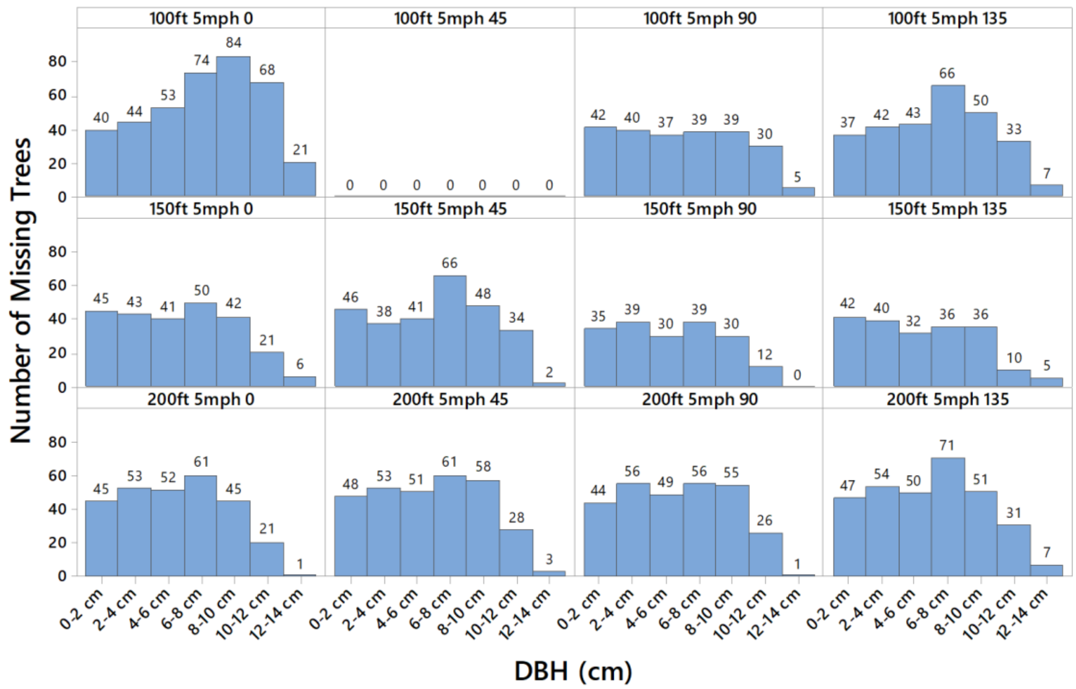

Figure 15. Frequency distribution of missing trees from automated tree detection by DBH class using orthoimages created by DroneDeploy

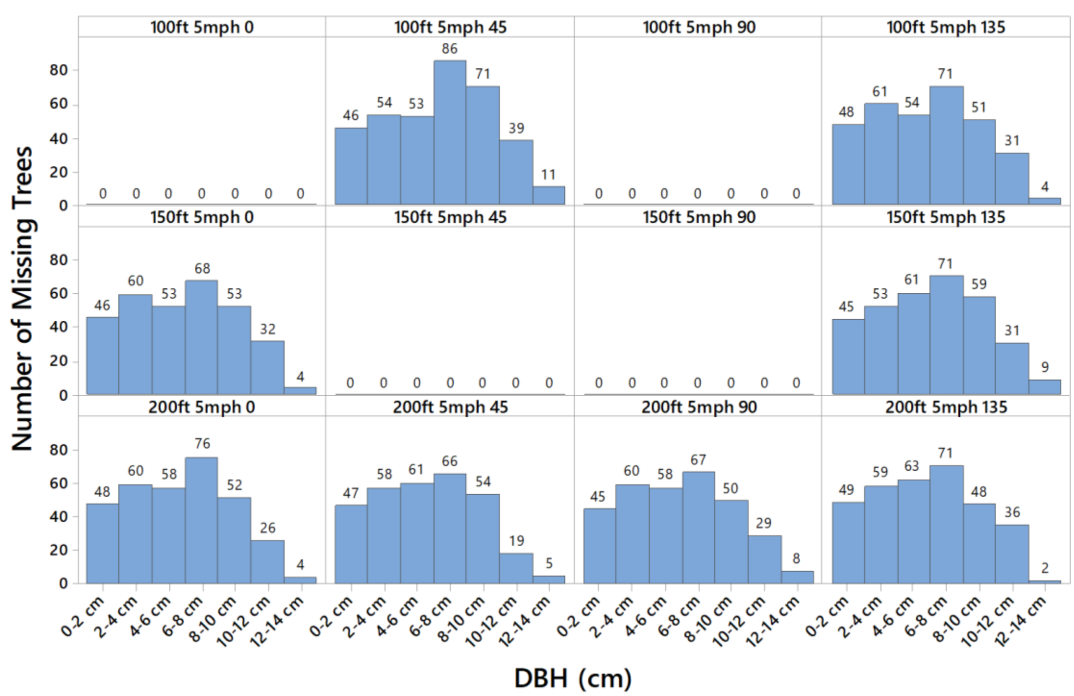

Figure 16. Frequency distribution of missing trees from automated tree detection by DBH class using orthoimages created by Agisoft

4.7. Positional Accuracy

The positional accuracy achieved by both the manual and automated tree detections were very good (Table 9). Manual detection has slightly better positional accuracy, with mean error around 0.5 m, as compared to automatic tree detection, which had fewer detected trees and a mean error of approximately 1.0 m. On average, mean positional error of DroneDeploy was 10 cm better than in Agisoft. The pattern in positional error varied among mission azimuths, with 135-degree missions having the lowest mean positional error at all flight altitudes.

The frequency distributions of positional error values from the manual tree detection of DroneDeploy orthoimages tended to be slightly right-skewed (Figure 17), particularly for 200 ft missions. In contrast, frequency distributions of positional error values showed no constant pattern for Agisoft orthoimages, with distributions being either uniform, right-skewed and left-skewed (Figure 18).

Excluding 200 ft missions, there were tree positional errors rarely greater than 1 m (Figure 17), while 100 and 150 ft orthoimagery often had tree locations greater than 1 m from the actual location. There was no pattern of mean positional error between missions with different azimuths.

On average, 92% of detected trees were located within their crown area, while there are only two missions in which this percentage drop between 70% and 85% (Table 10).

Table 9. Assessment of positional accuracy, based on distance between field- and image-tree coordinates

Procedure	Altitude (ft)	Hatch Angle	RMSE (m)		Mean distance (m)	
			DroneDeploy	Agisoft	DroneDeploy	Agisoft
Manual	100	0	0.60	N/A	0.53	N/A
		45	N/A	0.94	N/A	0.82
		90	0.69	N/A	0.63	N/A
		135	0.76	0.67	0.67	0.60
	150	0	0.64	0.75	0.59	0.63
		45	0.52	N/A	0.46	N/A
		90	0.67	N/A	0.62	N/A
		135	0.55	0.77	0.47	0.69
	200	0	0.56	0.73	0.49	0.65
		45	0.59	0.91	0.54	0.75
		90	0.57	0.75	0.52	0.64
		135	0.48	1.07	0.42	0.99
Automatic	100	0	4.32	N/A	1.36	N/A
		45	N/A	2.37	N/A	1.14
		90	1.13	N/A	0.95	N/A
		135	0.80	1.75	0.67	0.69
	150	0	4.31	1.10	0.91	0.86
		45	0.78	N/A	0.66	N/A
		90	3.08	N/A	0.77	N/A
		135	0.63	1.37	0.53	1.00
	200	0	5.15	0.88	1.07	0.80
		45	0.88	1.46	0.81	0.89
		90	1.36	2.06	0.77	0.78
		135	1.18	1.04	0.74	0.91

Table 10. Positional accuracy based on predicted image tree location falling within field crown area

Procedure	Altitude (ft)	Hatch Angle	DroneDeploy			Agisoft		
			Within half crown	Half to full crown	Outside of crown	Within Half crown	Half to full crown	Outside of crown
Manual	100	0	438	152	24	N/A	N/A	N/A
		45	N/A	N/A	N/A	252	251	86
		90	355	260	27	N/A	N/A	N/A
		135	376	206	68	386	227	28
	150	0	386	223	22	365	215	57
		45	499	117	14	N/A	N/A	N/A
		90	378	226	34	N/A	N/A	N/A
		135	485	135	30	312	251	52
	200	0	472	151	23	329	228	15
		45	432	185	16	278	259	69
		90	433	173	23	371	185	58
		135	541	89	13	144	324	143
Automatic	100	0	58	157	92	N/A	N/A	N/A
		45	N/A	N/A	N/A	126	171	37
		90	148	242	73	N/A	N/A	N/A
		135	251	125	41	277	81	17
	150	0	287	136	25	169	171	40
		45	261	134	26	N/A	N/A	N/A
		90	358	120	33	N/A	N/A	N/A
		135	363	106	26	113	200	52
	200	0	241	142	35	193	151	27
		45	167	203	24	171	182	32
		90	219	158	32	224	139	16
		135	216	151	18	142	179	47

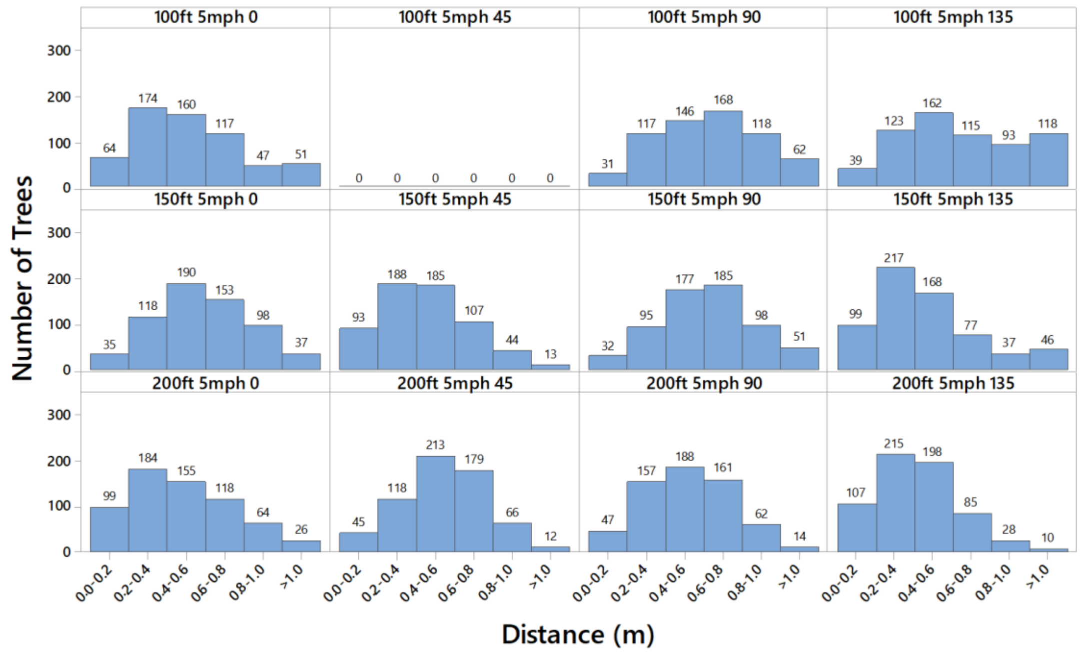

Figure 17. Histogram from manual tree detection displaying distribution of distance between field- and image-tree coordinates using orthoimage created by DroneDeploy

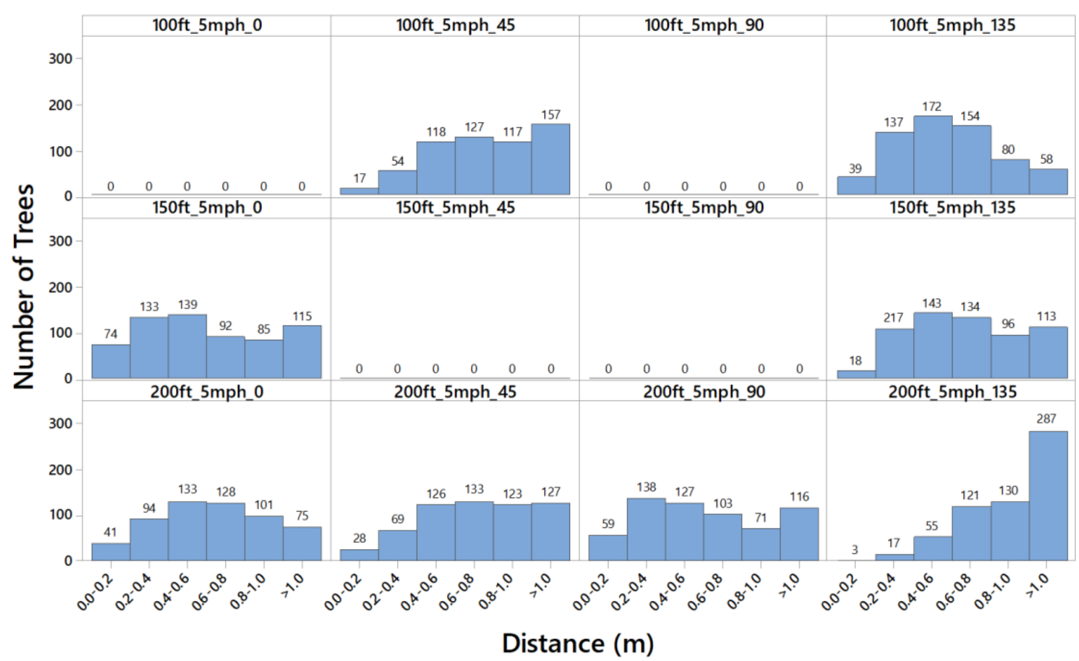

Figure 18. Histogram from manual tree detection displaying distribution of distance between field- and image-tree coordinates using orthoimage created by Agisoft

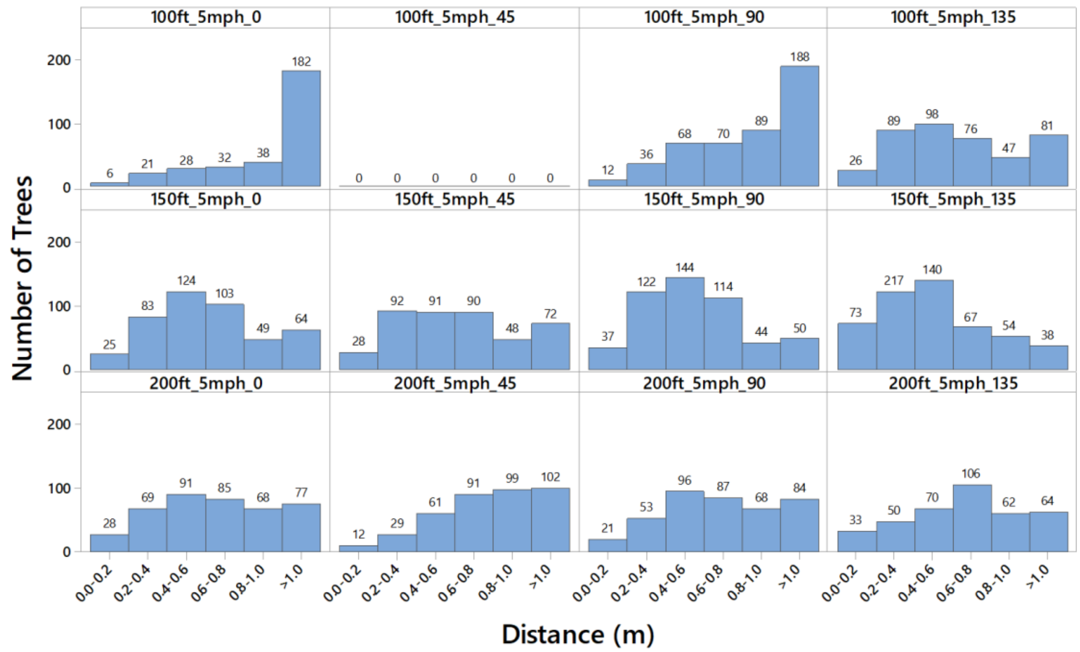

Figure 19. Histogram from autometad tree detection displaying distribution of distance between field- and image-tree coordinates using orthoimage created by DroneDeploy

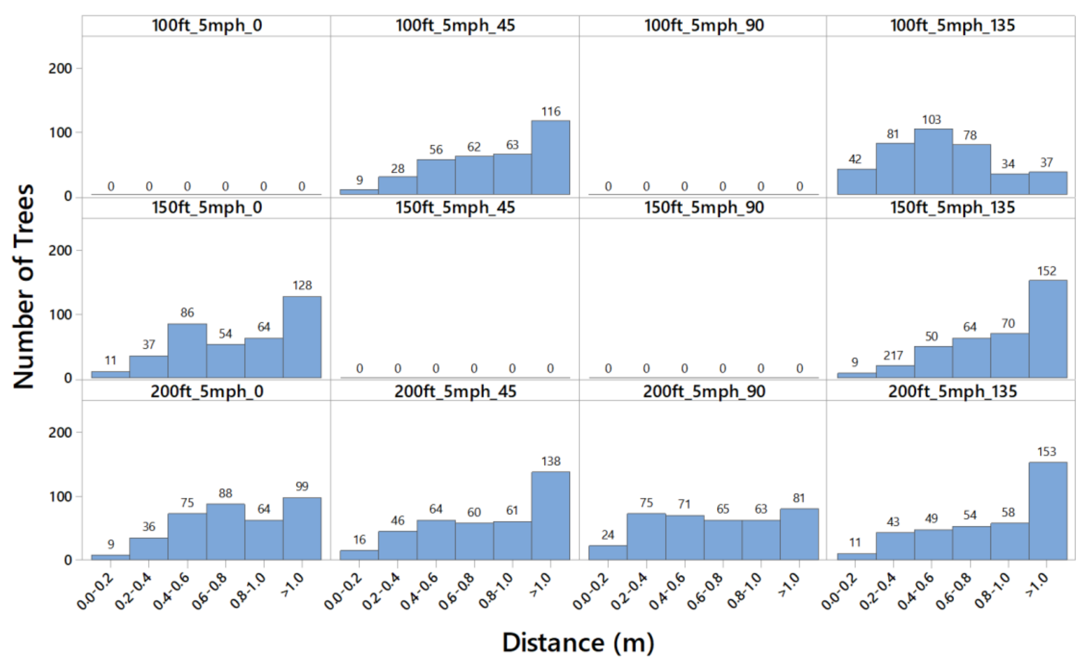

Figure 20. Histogram from autometad tree detection displaying distribution of distance between field- and image-tree coordinates using orthoimage created by Agisoft

4.8. Crown Delineation Accuracy

Crown Area (CA) determined from orthoimage matched the ground measurement with approximately 39.7% error for DroneDeploy and 53.3% error for Agisoft. CA derived from DroneDeploy was generally overestimated with mean error around 0.27 m^2, while CA derived from Agisoft was underestimated with mean error around -1.48 m^2.

Table 11. Assessment of crown delineation accuracy

Procedure	Altitude (ft)	Hatch Angle	Mean Difference (m^2)		RMSE (%)	
			DroneDeploy	Agisoft	DroneDeploy	Agisoft
Manual	100	0	0.00	N/A	43.51	N/A
		45	N/A	-0.64	N/A	51.65
		90	0.52	N/A	41.32	N/A
		135	0.49	-1.48	39.18	47.57
	150	0	-0.11	-1.71	38.30	56.79
		45	0.31	N/A	40.11	N/A
		90	0.15	N/A	36.33	N/A
		135	0.71	-1.48	35.55	49.83
	200	0	-0.04	-1.65	40.15	54.97
		45	0.21	-1.08	40.04	52.86
		90	0.12	-2.23	41.11	56.50
		135	0.56	-1.56	40.61	56.04

4.9. Relationship Between Field-Based and Imagery Derived Crown Area

From DroneDeploy, imagery derived crown area (CA) was found to have a positive, linear relationship with field-based crown area (Figure 21). The correlation with field-based CA has a R^2 of 64.62% and lowest RMSE of 1.92 m (Table 12). From Agisoft, there were generally weaker linear relationships between field and imagery CA estimates (Figure 22). The best model from Agisoft had a weaker relationship between field and imagery CA measurements compared to a worse model from DroneDeploy. Among all flight angles, the 135-degree azimuth flights produced imagery that provided better a relationship—i.e., stronger agreement—with field measurements.

With average slope value of 0.80, it suggests that imagery-based estimates tend to overestimate CA. This would be expected due to forced elliptical crown shape produced from imagery based estimates (Figure 7). This is clearly evident for larger trees, where the regression line lies beneath the 1:1 line (Figure 21 and Figure 22). This is not the case for smaller crown trees. In fact, CA estimates derived from Agisoft orthoimages are more likely to underestimate CA for smaller trees—i.e., regression line is above the 1:1 line.

DroneDeploy images produce better regression models, as evidenced by the larger R^2 and smaller RMSE fit statistics (Table 12), along with the tighter cluster of points near regression line on the scatter plots (Figure 21 and Figure 22). The scatter plots show larger scatter around regression line with larger CA. This suggest that the residuals have a heteroscedastic (cone-shape) distribution pattern.

Table 12. Detailed results from linear regression analyzes relating to image-based crown area and field-based crown area

Computer Program	Altitude (ft)	Hatch Angle	β0	β1	R^2 (%)	RMSE (m^2)
DroneDeploy	100	0	2.151	0.6624	45.22	2.37
		45	N/A	N/A	N/A	N/A
		90	1.376	0.7260	48.96	2.28
		135	0.934	0.7911	53.05	2.22
	150	0	1.190	0.8290	50.52	2.25
		45	1.534	0.7269	51.92	2.23
		90	0.706	0.8686	55.46	2.15
		135	0.640	0.8081	64.62	1.92
	200	0	1.435	0.7785	47.12	2.34
		45	1.429	0.7541	48.32	2.28
		90	1.675	0.7283	45.83	2.33
		135	1.173	0.7499	51.59	2.24
Agisoft	100	0	N/A	N/A	N/A	N/A
		45	3.004	0.5969	19.31	2.88
		90	N/A	N/A	N/A	N/A
		135	1.670	0.9607	41.86	2.44
	150	0	2.944	0.7358	19.30	2.90
		45	N/A	N/A	N/A	N/A
		90	N/A	N/A	N/A	N/A
		135	2.373	0.8202	37.46	2.56
	200	0	2.643	0.7952	24.65	2.83
		45	2.887	0.6644	18.63	2.90
		90	2.568	0.9198	34.76	2.55
		135	3.095	0.6824	19.63	2.90

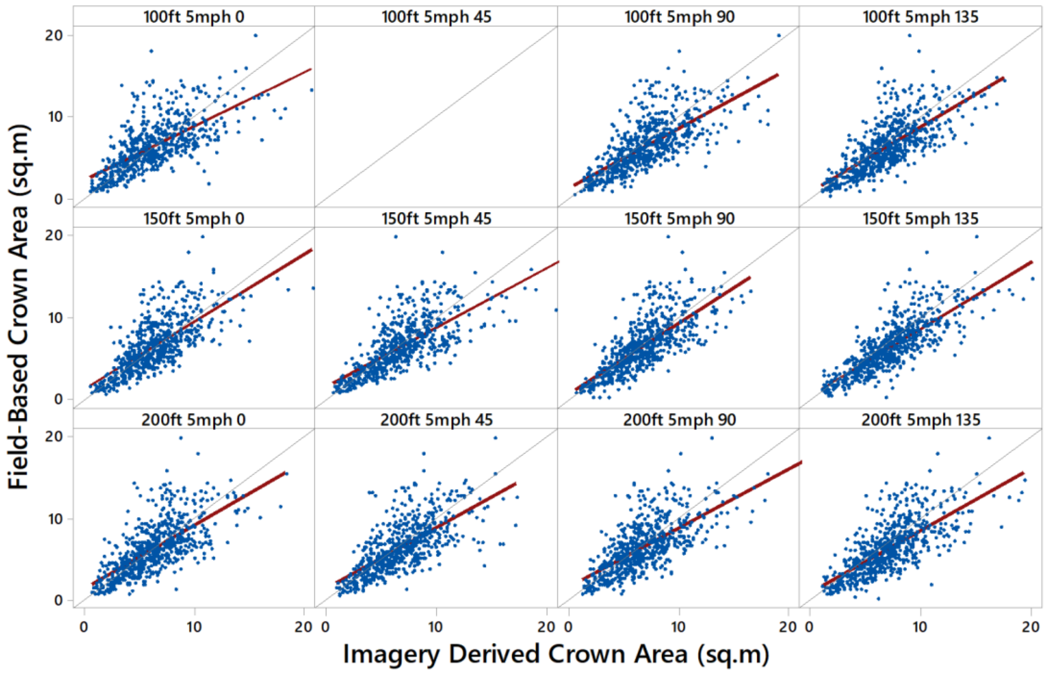

Figure 21. Scatter plot showing relationship in area between field- and image-tree crown using orthoimage created by DroneDeploy. Red line is regression equation, diagonal black line is a 1:1 identity reference

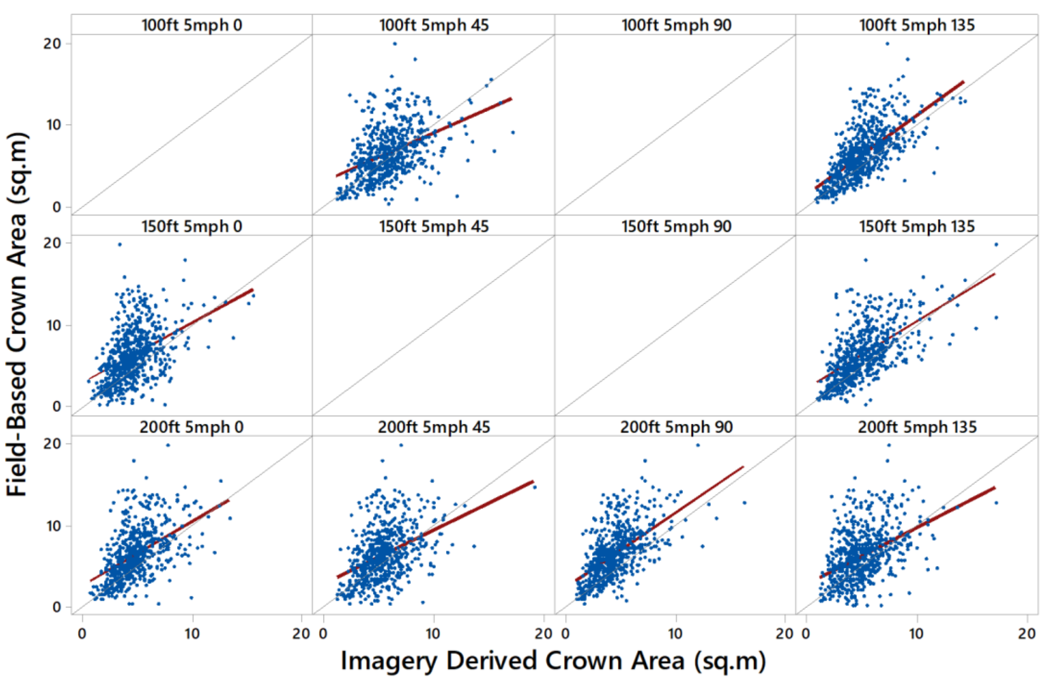

line.

Figure 22. Scatter plot showing relationship in area between field- and image-tree crown using orthoimage created by Agisoft. Red line is regression equation, diagonal black line is a 1:1 identity reference line.

4.9.1. Basal Area Relationship Between Field-Based Basal Area and Imagery Derived Crown Area

Similar to field and imagery crown area (CA) relationships, imagery derived CA from DroneDeploy was found to have a positive, linear relationship with between field measurements of basal area (BA) as compared to imagery derived CA from Agisoft which has weaker linear relationships (Table 13). The scatter plot shows points less spread out from DroneDeploy (Figure 23) as compare to the scatter plots from Agisoft (Figure 24). Among the different DroneDeploy images, there is more consistency in the estimated slopes from linear regression lines (Table 13), while the Agisoft images produced regression lines had greater variation in slope. However, similar to the CA:CA analysis (Figure 21 and Figure 22), residuals around regression line were not uniformly distributed, being smaller for smaller trees and increasing with tree size.

Table 13. Detailed results from linear regression analyzes relating to image-based crown and field-based basal area

Computer Program	Altitude (ft)	Hatch Angle	β0	β1	R^2 (%)	RMSE (cm^2)
DroneDeploy	100	0	0.000851	0.000764	46.29	26.72
		45	N/A	N/A	N/A	N/A
		90	-0.000277	0.000872	53.18	25.12
		135	-0.000591	0.000921	54.75	24.92
	150	0	-0.000450	0.000985	54.34	24.76
		45	0.000022	0.000858	55.43	24.52
		90	-0.000628	0.000973	53.11	25.20
		135	-0.000599	0.000890	59.44	23.54
	200	0	-0.000102	0.000919	49.24	26.29
		45	0.000015	0.000871	48.83	26.10
		90	0.000113	0.000869	49.25	25.97
		135	-0.000239	0.000861	51.95	25.60
Agisoft	100	0	N/A	N/A	N/A	N/A
		45	0.001338	0.000774	24.59	32.03
		90	N/A	N/A	N/A	N/A
		135	0.000187	0.001132	44.36	27.35
	150	0	0.001566	0.000897	21.88	32.68
		45	N/A	N/A	N/A	N/A
		90	N/A	N/A	N/A	N/A
		135	0.000982	0.000976	40.46	28.61
	200	0	0.001768	0.000852	21.57	33.06
		45	0.001306	0.000844	22.90	32.34
		90	0.001235	0.001087	36.37	29.12
		135	0.001937	0.000790	20.03	33.17

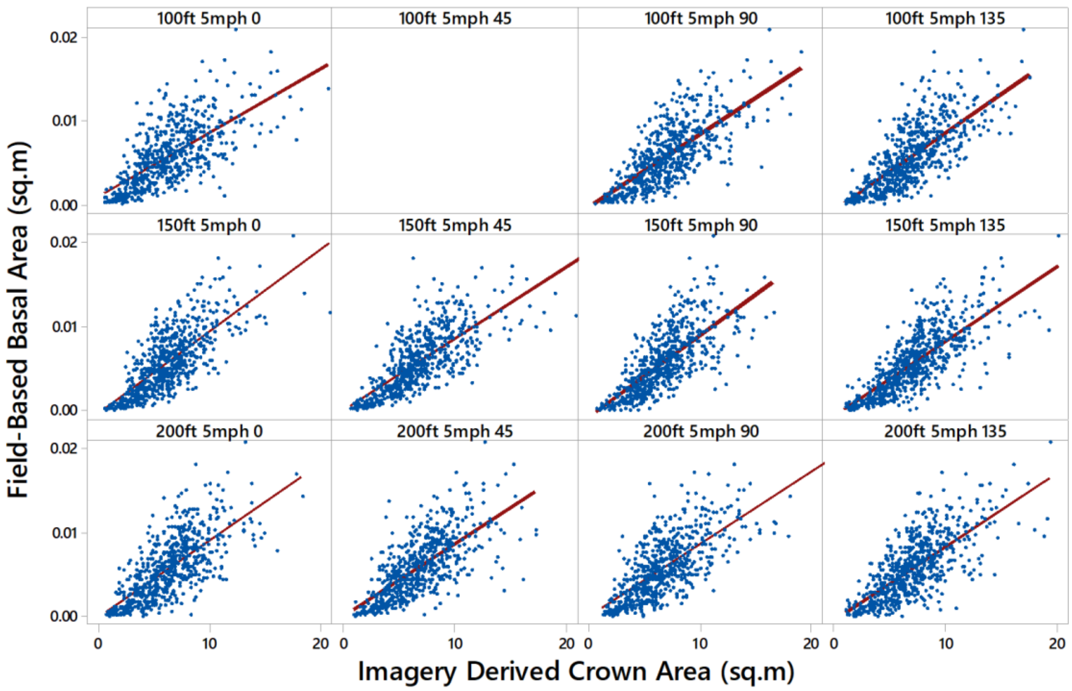

Figure 23. Scatter plot showing relationship in area between field-based basal area and image-tree crown using orthoimage created by DroneDeploy

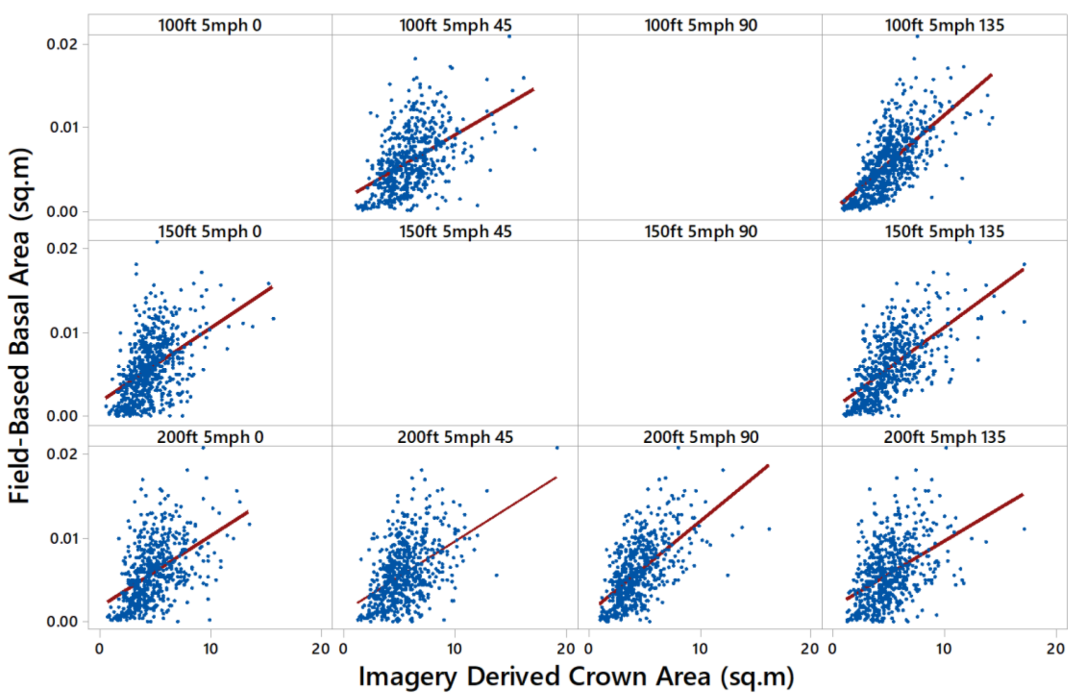

Figure 24. Scatter plot showing relationship in area between field-based basal area and image-tree crown using orthoimage created Agisoft

Chapter 5. DISCUSSION

Using UAVs for surveying forest regeneration has many advantages. Traditional field survey methods can take days or even weeks, but the same survey can be completed in hours by UAVs and the collected imagery can be processed on the same day. UAVs allow all kinds of payloads, such as RGB cameras to map surfaces. Not only do UAVs make the process cheaper and faster for inventory personnel, but they also make the job safer. In my field experience, for example, I stood on an underground bee nest and suffered multiple stings. Although there are advantages to using UAVs, there are still many challenges.

5.1. Challenges in acquiring UAV imagery

Creating a flight mission is relatively straight forward with most mission planning software or apps, and requires few user inputs. However, there can be some app issues. For example, to make all flights comparable with each other in terms of flight duration and number of images taken, the user can pre-program the UAV to repeat the exact flight area, changing only secondary inputs—i.e., flight orientation, speed, and altitude. In theory, flight mission data from the software can be stored in the internal storage of the tablet and then uploaded to the UAV in order to repeat mission parameters at any time. However, due to unknown reasons, pre-programming caused some significant inconsistencies on the UAV and caused it to follow an unexpected flight path (Figure 25). I assume it was caused by the Tower app itself and might be fixed with a future update. This glitch might not be an issue for other mission planning apps.

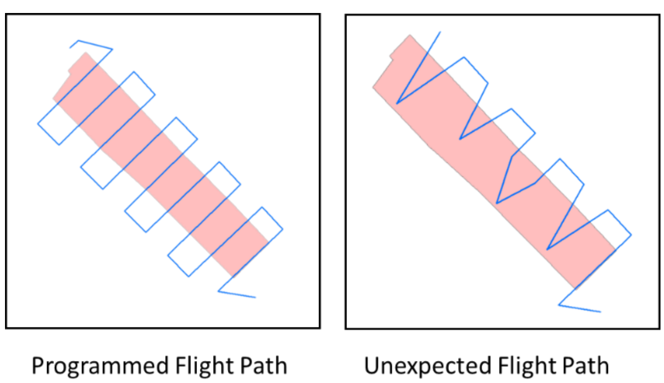

Figure 25. Example of unexpected flight path

A second challenge in image acquisition is data management. Missions flown during this study acquired, on average, up to 130 images and 4.5 GB of data on each camera. With more than one camera or even only one camera, file management of images is quite challenging after a couple of flights. I recommend that anyone attempting to conduct a large-area UAV survey requiring multiple missions—i.e., due to battery limitations—catalog all data immediately following each flight.

A third challenge is UAV image quality. Weather conditions have impact of UAV images. On overcast days, UAV imagery will have low reflectance values which greatly reduces data quality. Adjusting camera settings prior to each flight may improve image quality but requires detailed knowledge linking measures of cloudiness to camera settings. On intermittent cloudy days, a single mission may include both bright and dark images, impairing image analysis. In addition, windy days reduce or increase UAV speed depending on wind direction, increase battery consumption, and cause UAVs to loss stability, with pitch and role resulting in a great number of blurry pictures which were impossible to use. If I were to repeat my UAV flights, I would use a gimbal to see whether the quality of my results will improve.

5.2. Challenges in processing UAV imagery

5.2.1. Geotagging

Images must be geotagged before creating an orthoimage because MAPIR Survey 2 cameras do not geotag images during flight. This process requires downloading telemetry log (tlog) files which are recordings of a whole mission after connecting UAV with ground station (ArduPilot Dev Team, 2019). Due to tlog files not being a common format, they first needed to be converted into kml using MissionPlanner (ArduPilot, 2019). Following MAPIR guide (MAPIR Camera, 2015), all images can then be automatically geotagged using Geosetter (Schmidt, 2019).

Although all steps above were straight forward, I faced one challenge during geotagged images. When UAVs connected with ground station, it continues to record whole drone action without stopping between flight. This caused all survey path combined each other until ground station shut down (Figure 26) and caused a lot of confusion and trouble on matching images with corresponding flight path. This can be prevented resetting ground station after every flight.

Tlog from one flight path   Tlog from five combined flight path

Figure 26. Example of various tlogs output

5.2.2. Creating Orthomosaic

DroneDeploy (DroneDeploy, 2019) and Agisoft Metashape Professional (Agisoft, 2019) were used to create the orthoimages in this research. DroneDeploy can produce orthoimage after 1 to 3 hours of processing time, while Agisoft Metashape Professional needed between 15 to 22 hours. As this research included 48 (24 RGB and 24 IR) different flight missions, the whole process took about 45 days for Agisoft Metashape Professional while less than a week for DroneDeploy.

5.2.3. Creation of DEM

Using the same set of stereo images, both orthomosaic programs were inconsistent in the creation of Digital Elevation Model (DEM), and generated DEMs with very different characteristics of the crown surfaces. Crown shapes of individual trees from Agisoft had sharp edges and jagged shapes, which was in direct contrast to gradual and smooth edges of the crown surfaces produced in the DEM by DroneDeploy (Figure 27). The sharp edges in the DEM derived from Agisoft tend to create more errors of omission than those of DroneDeploy. This is because jagged crown surface will be cause some secondary maximum point within the same crown area which can be seen in Figure 27 which the crown surface created by Agisoft.

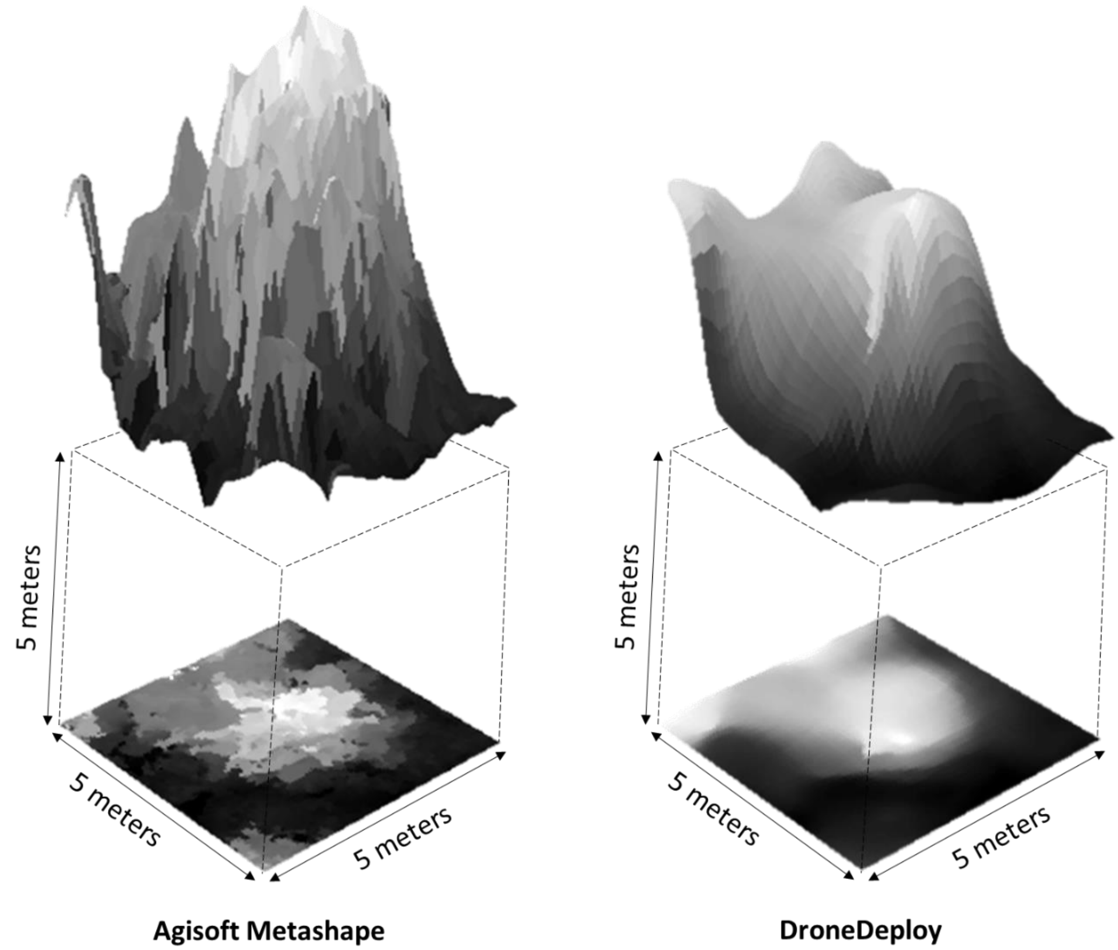

Figure 27. Two 3D surface models of crown shape from one individual tree, observed from same perspective, left image generated by Agisoft, right image by DroneDeploy

5.3. Imagery Analysis

5.3.1. Manual Tree Detection and Delineation

Individual tree detection from RGB Imagery is very accurate based the manual approach was used in this study. Tree identification success is very high, but it requires great amount of user input and time. For those trees correctly detected from the UAV data, the best performance was able to reach 93.1% detection accuracy (Table 7). With correctly detected trees, crown area estimates returned RMSEs of 39.7% and 53.3%, and mean difference of 0.26 m^2 (6.9%) and -1.48 m^2 (-20.2%) for DroneDeploy and Agisoft orthoimagery, respectively. These results are comparable to results obtained by Pouliot et al. (2002), who reported RMSE value of 11.2% and mean difference of -4.1%.

.

5.3.2. Automated Tree Detection

Numerous methods have been developed for individual tree detection using by lidar data. These methods either use Canopy Height Model (CHM) or point clouds. Even though CHM based approaches are considered to be not ideal due to some uncertainties involved during the interpolation process, there are commonly used (Lu, et al., 2014). It has been shown, however, that there are some limitations is this approached caused when there is uniform canopy structure and greatly overlapping tree crowns (Li, et al., 2012).

In this study, some existing tree detection algorithms were tested using DEMs derived from stereo UAV imagery as representing crown surfaces. Unfortunately, as these algorithms were developed for use with lidar derived CHM data, they could not able to create successful output for my stereo-image derived data. For further analysis, a model was built on using the local maxima approach to identify treetops in ArcMap model builder (Figure 28).

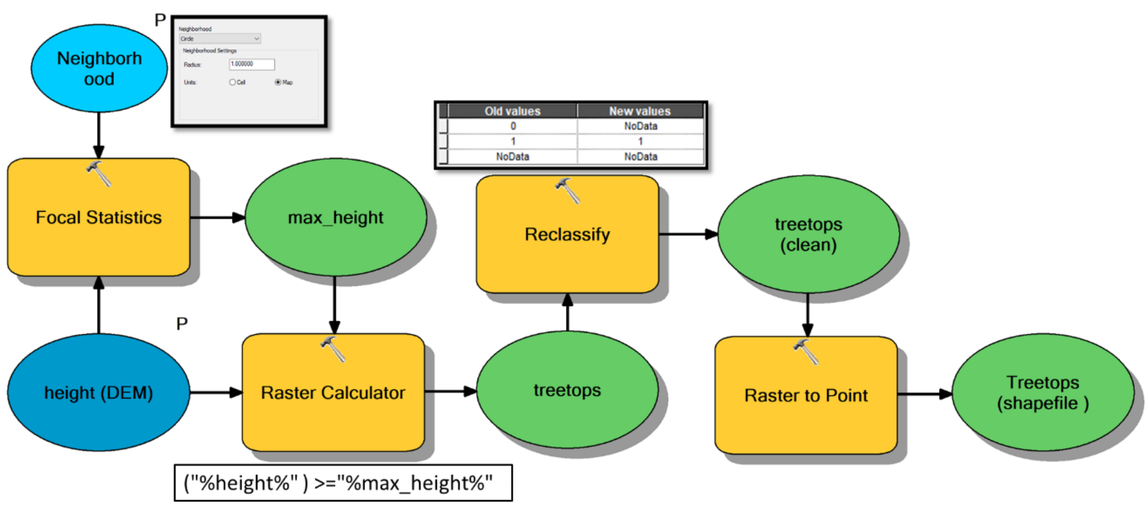

Figure 28. ArcMap model created for automated tree top detection from UAV digital elevation model.

The best result from the automated tree detection method was 63% success, with average success of 50% for DroneDeploy and 38% for Agisoft (Table 8). The number of correctly detected trees by automated approach was generally lower than values reported among other studies. Pitkänen et al. (2004), for example, used local maxima and several other methods to detect individual trees and only 40% of all trees were able to detected. In contrast, Korpela et al. (2007) applied the multi-scale template matching method and was able to achieve about 95% detection success. Näsi et al. (2015) performed watershed method and reported 74.7% detection accuracy. Additionally, Kattenborn et al. (2014) detected 86.1% of palm trees with Omission error = 9.4% and commission error = 5.4%. Also, Pouliot et al. (2002) reported 90.9% correctly detected trees.

In this study, the relatively poor performance of automated tree detection can be associated with the complex canopy structure of the Norway spruce crowns. Dense clusters of overlapping individual tree crowns of different sizes and shapes makes detection harder. The local maxima approach is based on the theory that trees are spaced sufficiently far apart so as to allow the CHM to accurately reflect the crown profile of a single treetop. With overtopped and overlapping tree crowns, some individual treetops did not appear as local maxima and could not be observed, while other local maxima caused by noise identified as source of error.

5.3.3. Resolution

Remote sensing data can be categorized in four primary types of resolution, namely spatial, spectral, radiometric, and temporal. Spatial resolution is typically defined as the size of a pixel along one side. Compared to the Landsat 8 has 30-meter spatial resolution, orthoimage created for this study has very high spatial resolution, averaging 1.1, 1.7, and 2.2 cm for 100, 150, and 200 ft flight altitudes, respectively. Spectral resolution is described as the number and width of individual spectral bands, or ranges of wavelength. For comparison, RGB images contain 3 bands, for red (wavelength between 630-680nm), green (520-590 nm) and blue (450-515 nm) visible light, while IR images have only 1 band (750-900 nm). From my data processing results, RGB images created more detailed and useful output—i.e., Orthoimage and DEM—as compared to IR images. However, I could not test if 4 band (RGB+IR) output would be an improvement over RGB output due to the two different cameras used acquiring data produced uncompilable picture. I assume that if I used a single camera that could record all 4 bands, my results could be slightly better. Radiometric resolution is described of capacity of information can be stored in one-pixel value as a unit of bits. The cameras used for this research has 24-bit which one pixel can have 16,777,215 (2^{24}) color levels. During post processing picture, 8-bit picture were produced but output quality produced from this picture is very low compare to the original pictures. Temporal resolution refers to time between measurement of same area. All data were acquired between 10 am and 4 pm in four different days. There were no statistical differences between same angle flights in term of temporal resolution.

Chapter 6. CONCLUSIONS

This research has demonstrated the potential for using UAV-based imagery for collecting information about forest regeneration. By using the same set of stereo images, the two photogrammetric software programs tested achieved significantly different results in terms of tree detection and crown delineation, with performance sometimes comparable but mostly not as strong as those achieved in other studies. However, individual tree detection using UAV-based DEM is still a relatively new research topic. Results suggest that not only will adjusting UAV mission parameters improve accuracies in tree detection and crown delineation, but that the choice of photogrammetric software used to generate orthoimagery and 3D canopy surface could improve results. While better results were obtained using manual approaches, improvements in automated approaches could increase their practicability.

Chapter 7. References

Agisoft, 2019. [Online]
Available at: https://www.agisoft.com/
[Accessed 2019].

Ameri, B., Meger, D., Power, K. & Gao, Y., 2009. UAS Applications: Disaster & Emergency Management. *American Society for Photogrammetry and Remote Sensing,* Volume 1, pp. 45-55.

Anon., 2020. *Picea abies.* [Online]
Available at: https://www.conifers.org/pi/Picea_abies.php

ArduPilot Dev Team, 2019. *Telemetry Logs.* [Online]
Available at: https://ardupilot.org/copter/docs/common-mission-planner-telemetry-logs.html
[Accessed 2020].

ArduPilot, 2019. *MissionPlanner,.* [Online]
Available at: https://github.com/ArduPilot/MissionPlanner

Austin, R., 2011. *Unmanned Aircraft Systems: UAVS Design, Development and Deployment.* s.l.:John Wiley & Sons.

Baier, R., Meyer, J. & Göttlein, A., 2007. Regeneration niches of Norway spruce (Picea abies [L.] Karst.) saplings in small canopy gaps in mixed mountain forests of the Bavarian Limestone Alps. *European Journal of Forest Research,* January , 126(1), pp. 11-22.

Boose, E. R., Boose, E. F. & Lezberg, A. L., 1998. A Practical Method for Mapping Trees Using Distance Measurements. *Ecology,* 79(3), pp. 819-827.

Brand, D. G., Leckie, D. G. & Cloney, E. E., 1991. Forest regeneration surveys: Design, data collection, and analysis. *The Forestry Chronicle,* 67(6), pp. 649-657.

Brandtberg, T., 1999. Automatic individual tree based analysis of high spatial resolution aerial images on naturally regenerated boreal forests. *Canadian Journal of Forest Research,* 29(10), pp. 1464-1478.

Brandtberg, T. & Walter, F., 1998a. Automated delineation of individual tree crowns in high spatial resolution aerial images by multiple-scale analysis. *Machine Vision and Applications,* Volume 11, p. 64–73.

Brandtberg, T. & Walter, F., 1998b. An algorithm for delineation of individual tree crowns in high spatial resolution aerial images using curved edge segments at multiple scales. *Automated Interpretation of High Spatial Resolution Digital Imagery for Forestry,* 10-12 February.pp. 41-54.

Briggs, R., 2001. *Svend O. Heiberg Memorial Forest Fact Sheet.* [Online] Available at: https://www.esf.edu/for/briggs/FOR345/heiberg.htm [Accessed 22 12 2018].

Chabot, D., 2018. Trends in drone research and applications as the Journal of Unmanned Vehicle Systems turns five. *Journal of Unmanned Vehicle Systems,* 6(1), pp. vi-xv.

Dănescu, A., Kohnle, U., Bauhus, J., Weiskittel, A., & Albrecht, A. T., 2018. Long-term development of natural regeneration in irregular, mixed stands of silver fir and Norway spruce. *Forest Ecology and Management,* 15 December, Volume 430, pp. 105-116.

Diaci, J., Kutnar, L., Rupel, M., Smolej, I., Urbancio, M., & Kraigher, H., 2000. Interactions of ecological factors and natural regeneration in an altimontane Norway spruce (Picea abies (L.) Karst.) stand. *Phyton (Horn, Austria),* 40(4), pp. 17-26.

DroidPlanner, 2016. *Tower.* [Online] Available at: https://github.com/DroidPlanner/Tower [Accessed 2019].

DroneDeploy, 2019. *DroneDeploy.* [Online] Available at: https://www.dronedeploy.com/

Erikson, M., 2003. Segmentation of individual tree crowns in colour aerial photographs using region growing supported by fuzzy rules. *Canadian Journal of Forest Research,* 33(8), p. 1557–1563.

ESF, n.d. *Heiberg Forest & Tully Field Station.* [Online] Available at: https://www.esf.edu/campuses/heiberg/ [Accessed 22 12 2018].

FAA, 2016. *SUMMARY OF SMALL UNMANNED AIRCRAFT RULE (PART 107).* [Online] Available at: https://www.faa.gov/uas/media/Part_107_Summary.pdf [Accessed 2020].

Göktoğan, A. H., Sukkarieh, S., Bryson, M., Randle, J., Lupton, T., & Hung, C., 2009. A Rotary-wing Unmanned Air Vehicle for Aquatic Weed Surveillance and Management. *Journal of Intelligent and Robotic Systems,* 57(1-4), pp. 467-484.

Goodbody, T. R., Coops, N. C., Hermosilla, T., Tompalski, P., & Crawford, P., 2018. Assessing the status of forest regeneration using digital aerial photogrammetry and unmanned aerial systems. *International Journal of Remote Sensing,* 39(15-16), pp. 5246-5264.

Goodbody, T. R., Coops, N. C., Marshall, P. L., Tompalski, P., & Crawford, P., 2017. Unmanned aerial systems for precision forest inventory purposes: A review and case study. *The Forestry Chronicle,* 93(1), pp. 71-81.

Hall, R. J. & Aldred, A. H., 1992. Forest regeneration appraisal with large-scale aerial photographs. *The Forestry Chronicle,* 68(1), pp. 142-150.

Heinzel, J. & Ginzler, C., 2019. A Single-Tree Processing Framework Using Terrestrial Laser Scanning Data for Detecting Forest Regeneration. *Remote Sensing,* 11(1), p. 60.

Hosley, N. W., 1936. Norway Spruce in the North-Eastern United States: A Study of Existing Plantations..

Jones IV, G. P., Pearlstine, L. G. & Percival, H. F., 2006. An Assessment of Small Unmanned Aerial Vehicles for Wildlife Research. *Wildlife Society Bulletin,* October, 34(3), pp. 750-758.

Juntunen, V. & Neuvonen, S., 2006a. Natural Regeneration of Scots Pine and Norway Spruce Close to the Timberline in Northern Finland. *Silva Fennica,* 40(3), p. 443–458.

Juntunen, V. & Neuvonen, S., 2006b. Predicting regeneration establishment in Norway spruce plantations using a multivariate multilevel model. *New Forests,* November, 32(3), p. 265–283.

Kattenborn, T., Sperlich, M., Bataua, K. & Koch, B., 2014. Automatic Single Palm Tree Detection in Plantations Using UAV-based Photogrammetric Point Clouds. *The International Archives of the Photogrammetry, Remote Sensing and Spatial Information Sciences,* 40(3), pp. 139-144.

Keane, J. A., 2004. *Natural regeneration of Norway spruce [Picea abies (L.) Karst.] within and around plantations in central New York,* Syracuse, New York: s.n.

King, D. J., 2000. Airborne remote sensing in forestry: Sensors, analysis and applications. *The Forestry Chronicle,* 76(6), pp. 859-876.

Kneppeck, I. D. & Ahern, F. J., 1987. *Evaluation of a multispectral linear array sensor for assessing juvenile stand conditions..* Ann Arbor, Michigan, International Symposium on Remote Sensing of Environment, pp. 955-969.

Korpela, I., Dahlin, B., Schäfer, H., Bruun, E., Haapaniemi, F., Honkasalo, J., Ilvesniemi, S., Kuutti, V., Linkosalmi, M., Mustonen, J. and Salo, M., 2007. Single-tree forest inventory using lidar and aerial images for 3D treetop positioning, species recognition, height and crown width estimation. *Int. Archieves Photogramm. Remote Sens.,* 36(3), pp. 227-233.

Larsen, M., 1997. *Crown modelling to find tree top positions in aerial photographs.* Copenhagen, Denmark, s.n.

LBM Journal, 2017. *Norway Spruce 101.* [Online]
Available at: https://lbmjournal.com/norway-spruce-101/

Leonard, R. T., 1985. *Forest floor and soil characteristics beneath Picea abies (L.) Karst. Stands in central New York,* Syracuse, New York: s.n.

Li, W., Guo, Q., Jakubowski, M. K. & Kelly, M., 2012. A New Method for Segmenting Individual Trees from the Lidar Point Cloud. *Photogrammetric Engineering & Remote Sensing,* January, 78(1), pp. 75-84.

Lu, X., Guo, Q., Li, W. & Flanagan, J., 2014. A bottom-up approach to segment individual deciduous trees usingleaf-off lidar point cloud data. *ISPRS Journal of Photogrammetry and Remote Sensing,* Volume 94, pp. 1-12.

MAPIR Camera, 2015. *Applying GPS Coordinates to Survey Images From an UAV Flight Log.* [Online]
Available at: https://www.youtube.com/watch?v=QXBNRqo6q8E

MAPIR CAMERA, 2020. *Camera Flight Calculator.* [Online]
Available at: https://www.mapir.camera/pages/camera-flight-calculator

Meyer, P., Janda, P., Mikoláš, M., Trotsiuk, V., Krumm, F., Mrhalová, H., Synek, M., Lábusová, J., Kraus, D., Brandes, J. and Svoboda, M., 2017. A matter of time: self-regulated tree regeneration in a natural Norway spruce (Picea abies) forest at Mt. Brocken, Germany. *European Journal of Forest Research,* December, 136(5-6), p. 907–921.

Näsi, R., Honkavaara, E., Lyytikäinen-Saarenmaa, P., Blomqvist, M., Litkey, P., Hakala, T., Viljanen, N., Kantola, T., Tanhuanpää, T. and Holopainen, M., 2015. Using UAV-Based Photogrammetry and Hyperspectral Imaging for Mapping Bark Beetle Damage at Tree-Level. *Remote sensing,* 18 November, Volume 7, pp. 15467-15493.

Panagiotidis, D., Abdollahnejad, A., Surový, P. & Chiteculo, V., 2017. Determining tree height and crown diameter from high resolution UAV imagery. *International Journal of Remote Sensing,* 38(8-10), pp. 2392-2410.

Pitkänen, J., Maltamo, M., Hyyppä, J. & Yu, X., 2004. Adaptive Methods for Individual Tree Detection on Airborne Laser. *International Archives of Photogrammetry, Remote Sensing and Spatial Information Sciences,* 36(8), pp. 187-191.

Pouliot, D. A., King, D. J., Bell, F. W. & Pitt, D. G., 2002. Automated tree crown detection and delineation in high-resolution digital camera imagery of coniferous forest regeneration. *Remote Sensing of Environment,* 82(2-3), pp. 322-334.

Puliti, S., Solberg, S. & Granhus, A., 2019. Use of UAV Photogrammetric Data for Estimation of Biophysical Properties in Forest Stands Under Regeneration. *Remote Sensing,* 11(3), p. 233.

Quilter, M. C. & Anderson, V. J., 2000. Low Altitude/Large Scale Aerial Photographs: A Tool ForRange And Resource Managers. *Rangelands Archives,* April, 22(2), pp. 13-17.

Quilter, M. C. & Anderson, V. J., 2001. A Proposed Method for Determining Shrub Utilization Using (LA/LS) Imagery. *Journal of Range Management,* 54(4), pp. 378-381.

Rango, A., Laliberte, A., Steele, C., Herrick, J.E., Bestelmeyer, B., Schmugge, T., Roanhorse, A. and Jenkins, V., 2006. Using Unmanned Aerial Vehicles for Rangelands: Current Applications and Future Potentials. *Environmental Practice,* 8(3), pp. 159-168.

Reynisson, V., 2011. Comparison of yield of Norway spruce (Picea abies) and Sitka spruce (Picea sitchensis) in Skorradalur, West Iceland..

Saari, H., Pellikka, I., Pesonen, L., Tuominen, S., Heikkilä, J., Holmlund, C., Mäkynen, J., Ojala, K. and Antila, T., 2011. *Unmanned Aerial Vehicle (UAV) operated spectral camera system for forest and agriculture applications.* s.l., s.n., p. 81740H.

Schmidt, F., 2019. *GEOSETTER.* [Online]
Available at: https://geosetter.de/en/main-en/
[Accessed 2019].

Siebert, S. & Teizer, J., 2014. Mobile 3D mapping for surveying earthwork projects using an Unmanned Aerial Vehicle (UAV) system. *Automation in Construction,* Volume 41, pp. 1-14.

Stein, W. I., 1992. Regeneration surveys and evaluation. In: s.l.:s.n., pp. 347-378.

Szydlarski, M. & Modrzyński, J., 2015. Increase of natural regeneration area of Norway spruce (Picea abies L. Karst.) in the Kaszuby Lake District during the decade 2002–2012. *Forest Research Papers,* March, 76(1), p. 66–72.

Thomas-Van Gundy, M. A., 1992. *White pine and Norway spruce under-plantings on the Charles Lathrop Pack Demonstration Forest.,* Syracuse, New York: s.n.

Watts, A. C., Ambrosia, V. G. & Hinkley, E. A., 2012. Unmanned Aircraft Systems in Remote Sensing and Scientific Research: Classification and Considerations of Use. *Remote Sensing,* 4(6), pp. 1671-1692.

Wood Products Development Council, 2017. *State Agriculture Commissioner Highlights New York's $23 Billion Forest Products Industry.* [Online]
Available at: https://woodproducts.ny.gov/news/state-agriculture-commissioner-highlights-new-yorks-23-billion-forest-products-industry

Woolsey, T. S. & Greeley, W. B., 1920. *Studies in French forestry.* s.l.:John Wiley and Sons, Inc..

W. R. C. C., 2007. *Period of Record Monthly Climate Summary.* [Online]
Available at: https://wrcc.dri.edu/cgi-bin/cliMAIN.pl?ny8627
[Accessed 22 12 2018].

Chapter 8. APPENDIX

Table 14. Complete list of field measurements

Tree No	Dbh (cm)	DGL (cm)	Height (m)	Crown (NS)	Crown (EW)	X Coordinate	Y Coordinate
1	11.9	17.4	6.29	3.117	2.842	411137.0843	4737160.997
2	14.8	20.7	7.61	4.074	3.908	411135.1456	4737159.466
3	11.6	16.1	6.86	3.380	3.296	411135.2414	4737162.812
4	7.5	10.3	5.37	2.706	2.874	411133.5425	4737160.916
5	6.2	8.4	5.22	2.656	2.484	411133.7383	4737164.690
6	8.1	10.1	6.28	3.182	3.214	411131.9221	4737163.156
7	1.1	2.4	1.88	1.182	1.096	411131.6888	4737159.616
8	11.0	16.6	6.65	3.938	3.964	411130.0449	4737157.944
9	11.1	14.9	6.86	3.562	3.460	411130.0127	4737161.282
10	7.6	8.5	5.95	2.912	2.821	411128.2910	4737159.665
11	5.6	9.3	6.86	3.566	3.242	411128.0977	4737156.278
12	10.8	14.4	6.14	3.266	3.236	411126.6809	4737161.511
13	14.2	17.5	9.32	3.588	3.158	411124.8028	4737159.755
14	13.3	17.9	7.77	4.291	3.956	411126.5664	4737154.745
15	7.8	10.2	6.70	3.118	3.148	411124.8071	4737156.543
16	2.4	4.3	2.94	1.471	1.448	411124.5494	4737153.066
17	12.0	16.3	7.92	3.754	3.704	411126.2088	4737151.315
18	10.5	14.4	7.35	3.578	3.298	411122.8903	4737154.745
19	8.2	11.0	5.62	2.722	2.648	411121.1757	4737153.172
20	11.5	15.1	6.84	4.060	3.946	411122.7660	4737147.887
21	2.8	4.5	3.10	1.544	1.684	411120.9112	4737146.199
22	10.7	14.6	6.36	4.054	3.666	411119.3223	4737148.021
23	12.8	17.5	7.13	3.564	3.423	411117.7125	4737149.836
24	8.2	10.7	5.74	2.872	3.090	411117.4408	4737146.423
25	12.3	15.5	8.08	3.418	3.192	411115.9380	4737148.242
26	11.0	13.2	6.21	4.584	4.403	411115.7492	4737144.726
27	1.2	2.9	2.14	1.096	1.038	411112.2806	4737144.864
28	11.9	15.7	8.40	4.060	4.002	411115.6257	4737141.392
29	8.2	10.9	6.05	2.896	2.769	411110.6249	4737146.750
30	6.4	8.2	6.48	2.252	2.982	411112.5071	4737148.353
31	9.4	12.5	6.99	2.856	3.114	411114.2717	4737150.016
32	5.7	7.5	5.91	2.136	2.528	411108.9745	4737148.604
33	13.2	19.6	6.41	4.104	4.072	411110.8370	4737150.154
34	9.9	12.4	7.47	2.802	3.064	411112.6193	4737151.810
35	12.3	14.4	7.64	3.602	4.580	411116.0706	4737151.522
36	11.9	16.4	7.79	4.122	4.246	411116.1051	4737154.970
37	12.6	17.1	8.84	3.198	3.278	411119.4168	4737154.874
38	8.6	9.4	6.57	2.252	2.451	411117.8566	4737156.694
39	12.9	18.5	8.36	5.192	4.380	411119.7314	4737158.387

Tree No	Dbh (cm)	DGL (cm)	Height (m)	Crown (NS)	Crown (EW)	X Coordinate	Y Coordinate
40	11.4	15.8	8.71	4.368	4.124	411123.0946	4737158.349
41	6.3	6.8	4.97	2.218	2.168	411121.6097	4737160.137
42	1.8	3.4	2.37	1.310	1.405	411125.0336	4737163.268
43	13.5	18.1	7.95	4.468	3.996	411128.5569	4737163.149
44	8.8	13.1	6.68	2.868	2.878	411130.2933	4737164.794
45	13.5	16.9	7.50	4.576	4.296	411131.9686	4737166.498
46	8.0	10.8	6.57	2.542	2.546	411128.5657	4737166.646
47	11.1	14.4	8.25	3.432	3.403	411126.7671	4737164.995
48	7.2	10.0	5.55	2.091	2.062	411128.7557	4737170.032
49	6.4	8.5	4.64	2.416	2.452	411126.8527	4737168.696
50	11.4	14.1	8.10	3.302	3.398	411125.1882	4737166.775
51	11.7	16.3	8.71	3.104	3.410	411123.4568	4737165.143
52	8.9	11.6	6.68	3.428	3.692	411121.3672	4737163.756
53	11.7	16.5	6.19	3.668	3.652	411119.7439	4737161.805
54	8.0	10.4	5.81	2.939	2.632	411117.8983	4737160.012
55	10.9	15.1	7.35	4.098	4.448	411116.1634	4737158.480
56	10.5	13.3	6.08	3.688	4.174	411114.3924	4737156.707
57	9.2	11.1	6.85	4.412	3.836	411112.8586	4737155.200
58	11.7	15.5	6.98	3.244	3.712	411110.8235	4737153.486
59	4.2	5.5	4.88	2.411	2.322	411109.2386	4737152.001
60	9.7	12.3	6.29	3.510	3.286	411107.3071	4737150.424
61	11.1	14.7	7.40	4.098	4.271	411105.7480	4737152.260
62	12.1	16.4	7.64	4.201	3.919	411107.7081	4737153.987
63	8.7	11.7	6.49	2.932	2.820	411110.9368	4737156.913
64	6.3	8.3	6.09	2.698	2.692	411112.6007	4737158.598
65	12.8	16.3	7.29	3.728	3.674	411114.4968	4737160.258
66	11.5	16.8	5.81	3.168	3.144	411118.0517	4737163.509
67	8.4	11.9	6.70	3.206	2.823	411119.5854	4737165.185
68	5.0	6.9	4.32	2.348	2.468	411121.5487	4737166.723
69	11.9	15.0	6.19	3.356	3.384	411123.6104	4737168.553
70	10.2	12.8	6.50	3.866	3.842	411125.2027	4737170.265
71	3.8	5.5	2.99	1.684	1.671	411127.0919	4737171.808
72	12.3	17.9	6.53	3.338	3.346	411125.3698	4737173.701
73	9.9	12.8	6.47	2.801	3.513	411123.7052	4737172.110
74	9.1	11.8	6.82	3.302	3.141	411120.0694	4737168.904
75	10.9	14.5	8.25	3.246	3.044	411118.1953	4737167.209
76	8.5	11.1	6.58	2.852	3.319	411116.4745	4737165.160
77	10.4	14.2	7.64	2.912	3.358	411114.3265	4737163.814
78	7.8	12.1	6.34	3.042	2.834	411110.9467	4737160.261
79	8.0	11.6	7.00	2.528	2.376	411109.5758	4737158.435
80	7.4	10.5	5.92	2.580	2.272	411104.1691	4737157.210
81	10.0	14.3	8.25	3.292	3.436	411105.7924	4737158.857
82	11.6	15.1	8.10	3.369	3.368	411107.5925	4737160.736

Tree No	Dbh (cm)	DGL (cm)	Height (m)	Crown (NS)	Crown (EW)	X Coordinate	Y Coordinate
83	8.1	10.7	7.33	3.168	2.952	411109.3823	4737162.147
84	8.8	11.4	7.41	2.642	2.736	411111.0470	4737163.866
85	9.1	12.3	7.22	3.362	3.466	411112.8975	4737165.470
86	14.1	18.5	8.40	3.186	3.882	411114.7221	4737167.000
87	12.2	17.4	8.10	3.694	3.946	411116.6087	4737169.010
88	14.1	18.8	6.94	4.104	3.871	411120.4172	4737172.210
89	7.9	10.3	5.94	2.542	2.359	411122.0650	4737173.966
90	4.0	6.0	3.96	1.742	1.714	411123.7972	4737175.481
91	13.1	19.5	8.25	3.922	4.152	411120.5389	4737175.658
92	10.3	15.1	6.07	4.194	3.898	411118.6059	4737173.853
93	8.4	11.6	6.49	3.342	3.122	411117.0420	4737172.478
94	11.3	15.5	7.64	4.092	3.964	411115.0151	4737170.960
95	10.8	14.1	6.39	3.264	3.192	411113.2577	4737168.753
96	3.6	5.4	3.82	1.950	1.914	411111.2649	4737167.169
97	6.7	10.6	5.46	2.678	2.870	411109.4408	4737165.590
98	1.0	2.8	1.77	0.948	0.804	411104.0624	4737160.561
99	6.4	9.1	4.64	2.368	2.528	411099.0799	4737159.217
100	2.9	4.5	2.54	1.324	1.252	411100.8587	4737160.847
101	4.7	6.2	4.15	1.952	2.016	411102.5105	4737162.337
102	11.8	15.7	7.95	3.198	3.220	411103.9284	4737163.971
103	10.8	14.5	7.79	2.980	3.038	411105.8569	4737165.685
104	9.2	14.2	7.22	2.876	2.845	411107.7355	4737167.268
105	9.6	13.8	7.46	3.062	3.036	411109.4932	4737169.006
106	11.7	16.1	7.79	4.108	4.422	411111.4946	4737170.531
107	11.0	14.5	6.78	3.336	3.350	411113.1919	4737172.238
108	7.4	10.1	6.18	2.331	2.242	411115.4783	4737174.204
109	2.8	5.0	3.04	1.536	1.580	411117.0645	4737175.737
110	6.9	9.3	5.03	2.764	2.892	411118.7079	4737177.571
111	2.2	4.4	2.44	1.376	1.452	411120.5932	4737179.083
112	11.8	15.7	6.46	3.339	3.228	411118.7545	4737180.786
113	10.7	15.1	6.97	3.262	3.442	411117.0606	4737179.116
114	13.9	19.2	7.95	4.366	4.195	411115.1507	4737177.390
115	10.2	15.1	7.52	3.336	3.534	411113.6605	4737175.901
116	9.5	15.4	6.54	3.424	3.224	411111.6461	4737174.382
117	7.7	10.8	6.60	2.636	2.505	411109.8192	4737172.415
118	9.1	14.0	5.26	3.474	3.672	411106.0421	4737169.189
119	8.0	10.7	5.73	3.130	3.298	411104.3889	4737167.580
120	9.0	12.9	7.52	3.292	3.380	411102.6297	4737165.863
121	8.7	12.0	5.98	3.336	3.122	411099.1588	4737162.591
122	3.9	6.9	3.81	1.820	1.674	411097.2634	4737160.821
123	5.6	8.6	4.54	2.200	2.166	411097.3778	4737164.319
124	10.4	13.8	8.40	3.084	2.984	411099.0168	4737166.003
125	10.5	13.6	6.58	3.518	3.380	411101.0700	4737167.256

Tree No	Dbh (cm)	DGL (cm)	Height (m)	Crown (NS)	Crown (EW)	X Coordinate	Y Coordinate
126	10.5	14.1	6.88	3.164	3.112	411102.6984	4737169.273
127	8.3	12.3	5.40	3.422	3.134	411106.1837	4737172.661
128	8.2	11.5	6.05	2.914	2.764	411108.0278	4737174.272
129	11.4	15.2	7.79	3.878	3.038	411111.7886	4737177.471
130	3.9	5.6	4.03	2.080	2.168	411113.5529	4737179.021
131	7.6	11.4	4.80	2.570	2.584	411115.4670	4737180.836
132	10.2	13.2	7.01	2.702	2.590	411117.0415	4737182.534
133	12.6	17.3	7.79	3.680	3.526	411115.3300	4737184.144
134	13.9	18.8	7.95	3.916	3.896	411113.6468	4737182.485
135	11.4	15.4	7.79	2.912	3.008	411111.8399	4737180.793
136	11.7	16.1	7.95	3.562	3.732	411110.1932	4737179.268
137	6.8	10.8	5.55	2.442	2.364	411108.2320	4737177.783
138	5.4	8.4	4.76	1.976	1.832	411106.3705	4737176.093
139	9.6	14.4	5.01	3.353	3.385	411102.7801	4737172.726
140	3.3	4.8	2.96	1.386	1.476	411100.7807	4737170.999
141	2.1	4.8	2.81	1.624	1.688	411099.2750	4737169.626
142	4.7	8.3	4.82	2.670	2.553	411097.3968	4737167.863
143	10.9	15.2	7.95	3.222	2.972	411095.7328	4737166.152
144	5.6	9.7	4.58	2.098	2.112	411093.7488	4737164.428
145	5.2	7.8	4.68	2.586	2.503	411094.1597	4737167.839
146	8.0	11.2	6.45	2.794	2.946	411095.7210	4737169.554
147	7.5	12.2	5.17	2.892	2.762	411099.1480	4737172.829
148	4.3	7.6	3.51	2.092	1.786	411102.6259	4737176.176
149	3.5	5.6	3.27	1.920	1.720	411104.6363	4737177.908
150	7.6	10.0	6.11	2.626	2.762	411106.6180	4737179.461
151	6.6	9.0	5.28	2.536	2.210	411108.4909	4737181.050
152	12.4	17.8	6.29	3.722	4.076	411110.1845	4737182.620
153	8.2	11.4	5.64	2.776	2.935	411112.2477	4737187.631
154	9.3	12.9	6.20	2.912	2.838	411110.3780	4737186.151
155	5.0	6.4	4.28	1.962	2.060	411108.3196	4737184.581
156	5.7	7.7	5.58	2.630	2.358	411106.6046	4737182.833
157	6.5	11.5	4.89	2.776	2.643	411102.9382	4737179.572
158	7.7	10.5	5.55	2.412	2.634	411101.0514	4737177.919
159	3.4	5.8	3.50	1.536	1.514	411097.5821	4737174.460
160	2.8	5.3	2.81	1.756	1.516	411095.8310	4737172.935
161	6.5	10.1	5.89	2.208	2.394	411094.0269	4737171.407
162	10.2	14.3	8.10	3.424	3.272	411092.3461	4737169.604
163	11.1	18.6	8.10	3.748	3.610	411090.4565	4737167.930
164	6.4	9.8	5.28	2.465	2.364	411088.6897	4737169.724
165	9.9	14.9	7.95	3.046	2.784	411090.6497	4737171.365
166	11.0	14.7	6.10	3.362	3.212	411092.3633	4737173.074
167	8.9	13.6	6.88	2.902	2.792	411094.1838	4737174.629
168	8.0	10.7	6.77	2.992	3.074	411095.6767	4737176.371

Tree No	Dbh (cm)	DGL (cm)	Height (m)	Crown (NS)	Crown (EW)	X Coordinate	Y Coordinate
169	10.2	15.5	6.14	3.064	3.172	411099.3758	4737179.827
170	6.3	8.8	5.17	2.626	2.520	411101.3234	4737181.414
171	4.6	6.8	4.16	2.466	2.150	411105.1708	4737184.630
172	3.5	4.7	4.09	1.834	1.750	411106.6557	4737186.187
173	9.9	15.8	6.71	3.576	3.436	411108.6052	4737187.878
174	9.2	11.8	7.64	3.670	3.334	411110.4845	4737189.463
175	8.7	12.8	6.64	3.176	3.002	411108.7928	4737191.226
176	2.4	4.1	3.02	1.184	1.216	411106.7629	4737189.801
177	10.6	15.3	7.17	3.654	3.446	411105.1052	4737188.033
178	10.2	14.1	7.64	4.242	3.904	411103.2915	4737186.170
179	9.1	12.7	6.21	3.144	3.360	411099.6914	4737183.292
180	4.7	9.2	3.83	2.256	2.176	411097.6636	4737181.620
181	7.6	11.9	6.63	2.796	2.984	411094.0634	4737178.052
182	9.6	13.3	5.32	3.412	3.204	411090.5823	4737174.876
183	10.0	14.4	7.95	3.362	3.448	411089.0654	4737173.038
184	7.1	11.4	5.04	2.794	2.618	411087.1193	4737171.498
185	9.0	12.0	5.61	3.290	3.100	411085.4027	4737173.286
186	2.6	3.8	2.98	1.258	1.296	411088.9338	4737176.717
187	10.3	15.5	4.88	4.144	3.952	411090.7297	4737178.278
188	2.6	4.3	3.12	1.278	1.522	411092.3957	4737179.675
189	8.3	13.4	6.37	2.370	2.306	411094.3332	4737181.655
190	7.6	11.9	5.55	2.484	2.470	411096.0217	4737183.373
191	11.5	16.6	5.89	4.082	3.450	411098.0724	4737185.021
192	10.9	16.9	6.15	3.340	3.226	411099.8200	4737186.619
193	6.9	10.3	5.45	2.650	2.320	411101.6916	4737188.107
194	10.5	14.6	7.64	2.910	3.096	411103.4979	4737189.762
195	8.7	13.1	5.60	2.844	2.764	411107.2036	4737192.923
196	7.2	12.2	5.00	2.780	2.470	411105.7648	4737194.446
197	2.7	4.9	3.03	1.608	1.426	411103.8224	4737193.152
198	9.6	12.3	6.36	3.178	3.292	411101.8108	4737191.666
199	12.2	19.8	7.46	3.741	3.692	411099.8847	4737189.860
200	13.0	19.5	7.02	4.518	3.868	411096.4344	4737186.822
201	11.2	16.4	7.79	3.852	3.712	411094.5117	4737185.211
202	2.7	6.1	3.14	1.554	1.548	411092.5139	4737183.468
203	7.5	11.6	6.32	2.546	2.242	411089.0261	4737180.020
204	9.3	13.8	6.48	2.892	3.122	411087.3275	4737178.503
205	4.8	7.6	4.55	1.826	1.938	411083.6565	4737175.078
206	1.5	3.2	2.16	1.074	1.122	411081.9528	4737176.857
207	5.9	8.2	5.21	2.226	2.176	411083.9628	4737178.573
208	8.6	13.3	6.09	3.048	2.902	411085.5961	4737180.144
209	12.0	17.2	6.78	3.514	3.816	411087.3009	4737181.789
210	8.0	11.5	4.45	3.420	3.112	411088.6635	4737183.729
211	8.2	11.8	5.91	2.714	2.516	411091.0847	4737185.246

Tree No	Dbh (cm)	DGL (cm)	Height (m)	Crown (NS)	Crown (EW)	X Coordinate	Y Coordinate
212	7.0	10.5	5.03	2.342	2.186	411092.9031	4737187.029
213	13.7	19.2	5.45	4.092	3.860	411094.7235	4737188.640
214	11.6	16.4	6.00	4.052	3.810	411096.6005	4737190.174
215	8.3	11.4	6.14	2.594	2.732	411098.1536	4737191.699
216	2.0	4.4	3.12	1.232	1.276	411100.2129	4737193.482
217	9.2	13.3	6.40	3.314	2.906	411103.9810	4737196.650
218	8.6	14.3	5.73	3.348	3.120	411098.4591	4737195.188
219	4.4	7.7	3.81	1.930	1.916	411096.6804	4737193.439
220	7.9	13.0	6.06	2.716	2.652	411094.8048	4737191.971
221	1.2	2.8	1.78	1.476	1.214	411093.0106	4737190.417
222	0.9	2.6	1.62	1.062	1.050	411091.3184	4737188.872
223	12.4	18.6	5.81	4.052	4.332	411085.6453	4737183.601
224	10.1	14.8	7.03	3.938	4.017	411083.9539	4737182.041
225	7.4	12.1	5.75	2.672	2.743	411082.2056	4737180.296
226	6.6	11.5	5.36	2.630	2.654	411080.3775	4737178.650
227	7.0	9.9	5.85	2.514	2.436	411078.7137	4737180.422
228	7.4	12.3	4.89	2.878	2.610	411084.0142	4737185.435
229	2.8	4.6	3.15	1.746	1.686	411089.6912	4737190.582
230	2.0	3.9	2.17	1.205	1.258	411091.2571	4737192.232
231	3.0	6.3	3.20	1.560	1.414	411093.1971	4737193.758
232	2.4	3.9	2.87	1.376	1.383	411096.7485	4737197.102
233	10.3	15.2	6.62	3.206	2.956	411098.7593	4737198.746
234	8.2	12.8	5.48	2.532	2.634	411098.9349	4737201.977
235	10.1	16.0	7.12	3.022	3.196	411097.0157	4737200.489
236	4.7	8.8	3.81	2.240	2.358	411094.9729	4737198.736
237	13.4	18.7	6.69	3.208	3.572	411093.4669	4737197.174
238	5.6	7.7	3.80	1.766	1.892	411089.6388	4737193.867
239	2.6	5.7	2.81	1.332	1.412	411088.1170	4737192.233
240	10.3	16.5	5.06	3.852	3.638	411082.2470	4737187.396
241	3.5	6.5	3.57	1.658	1.558	411080.8636	4737185.363
242	4.1	8.1	4.26	2.344	2.412	411075.6990	4737183.526
243	10.8	15.6	6.28	3.404	3.327	411075.5716	4737187.391
244	6.8	10.2	5.16	2.548	2.561	411077.3509	4737189.092
245	0.6	2.4	1.46	0.744	0.628	411079.0604	4737190.895
246	10.4	15.3	6.31	3.148	3.093	411082.5475	4737190.579
247	16.3	21.5	6.80	4.461	4.220	411086.1597	4737194.248
248	9.9	14.1	5.69	3.185	2.734	411087.8691	4737195.777
249	8.2	12.9	7.10	2.652	2.624	411084.3850	4737196.130
250	9.7	12.9	5.26	3.002	2.994	411086.2258	4737197.548
251	5.9	8.9	5.11	2.504	2.720	411088.5655	4737198.638
252	8.3	13.3	5.94	2.516	2.552	411091.8030	4737198.998
253	6.1	9.4	4.96	2.276	2.204	411089.9512	4737200.746
254	10.6	16.8	6.25	3.268	3.140	411093.5009	4737200.615

Tree No	Dbh (cm)	DGL (cm)	Height (m)	Crown (NS)	Crown (EW)	X Coordinate	Y Coordinate
255	2.4	5.2	2.57	1.496	1.484	411091.7463	4737202.351
256	7.1	10.4	5.32	2.930	3.016	411093.7386	4737204.014
257	10.0	17.6	6.19	3.626	3.570	411097.1319	4737203.881
258	9.5	15.1	6.55	3.402	3.435	411095.6488	4737205.416
259	7.5	13.1	4.83	2.610	2.762	411088.3696	4737202.652
260	5.9	8.8	4.26	2.258	1.896	411091.9287	4737205.852
261	7.5	12.0	4.82	2.756	2.704	411094.0474	4737207.255
262	6.5	9.4	5.23	2.216	2.214	411084.6502	4737199.382
263	4.9	7.5	4.43	1.748	1.928	411081.1231	4737196.020
264	12.8	19.2	7.79	3.278	3.236	411079.2998	4737194.229
265	5.0	7.1	5.02	1.756	1.958	411077.4886	4737192.680
266	10.0	14.9	7.48	3.682	3.505	411075.6937	4737190.927
267	12.3	17.9	7.26	4.218	4.030	411074.0402	4737189.131
268	6.6	10.9	5.37	2.424	2.538	411071.9993	4737187.480
269	0.0	1.1	0.93	0.632	0.678	411073.7997	4737185.420
270	10.7	14.9	7.79	2.954	3.218	411072.3465	4737190.967
271	5.7	8.5	4.98	1.856	1.962	411075.7027	4737194.407
272	9.3	13.8	7.64	2.956	2.932	411077.5841	4737196.048
273	10.9	15.6	7.73	3.108	2.986	411079.4541	4737197.805
274	9.9	13.3	5.78	2.872	2.864	411081.1927	4737199.651
275	8.8	12.0	7.54	2.565	2.838	411083.0452	4737201.094
276	11.2	15.8	6.16	3.522	3.468	411084.8983	4737202.890
277	6.2	9.7	4.15	2.108	2.212	411086.6935	4737204.346
278	4.4	8.1	4.05	1.694	1.404	411088.5676	4737205.975
279	6.7	11.7	4.55	2.524	2.560	411092.3679	4737209.067
280	8.5	12.3	6.04	2.920	3.092	411085.1222	4737206.312
281	0.7	2.4	1.51	0.942	0.996	411086.9782	4737207.791
282	9.1	13.0	5.83	1.906	2.550	411088.5773	4737209.422
283	4.6	7.1	4.11	2.216	1.762	411090.8676	4737210.746
284	10.3	14.9	6.91	3.026	2.694	411081.4604	4737203.061
285	0.0	1.6	0.86	0.548	0.580	411077.8681	4737199.602
286	0.6	2.3	1.64	1.290	1.032	411090.4056	4737207.761
287	0.0	1.7	0.98	0.736	0.742	411075.7976	4737198.065
288	10.5	14.7	7.48	3.730	3.626	411074.0228	4737196.307
289	9.5	14.1	6.40	3.054	3.182	411072.2795	4737194.542
290	10.3	14.7	7.42	2.486	2.764	411070.7311	4737192.800
291	9.2	13.0	7.32	3.446	3.394	411069.0456	4737194.685
292	9.6	13.2	5.87	3.026	2.984	411070.7349	4737196.297
293	13.7	18.2	7.70	4.164	3.986	411072.5099	4737197.977
294	3.1	5.3	3.46	1.992	1.744	411074.3756	4737199.570
295	7.4	11.4	6.52	3.004	3.160	411076.2813	4737201.420
296	9.0	13.1	5.92	3.030	3.004	411077.8084	4737203.277
297	9.0	15.0	4.50	3.446	3.318	411079.7637	4737204.786

Tree No	Dbh (cm)	DGL (cm)	Height (m)	Crown (NS)	Crown (EW)	X Coordinate	Y Coordinate
298	5.3	9.6	3.97	2.272	2.204	411083.3452	4737207.950
299	1.7	4.3	1.96	1.085	1.136	411084.9513	4737209.847
300	9.1	13.1	6.66	2.964	2.648	411083.5346	4737211.431
301	10.5	15.2	5.82	3.296	2.818	411085.2668	4737212.985
302	4.6	7.9	4.11	1.726	1.860	411087.4350	4737214.572
303	10.1	14.1	7.54	3.052	2.816	411081.7112	4737209.767
304	0.0	1.9	1.07	0.582	0.720	411079.8985	4737208.068
305	3.7	6.7	3.69	1.730	1.790	411077.9310	4737206.511
306	8.2	12.8	6.50	2.996	3.120	411076.2068	4737205.000
307	10.4	14.6	5.81	3.112	2.760	411074.5117	4737203.176
308	7.6	11.6	5.00	2.796	2.836	411072.6870	4737201.362
309	7.6	12.5	5.32	2.354	2.442	411070.8421	4737199.848
310	7.5	10.2	4.68	2.724	2.394	411069.1972	4737198.013
311	6.9	10.1	5.82	3.010	2.644	411067.4544	4737196.364
312	7.5	11.3	6.07	2.332	2.534	411065.6297	4737194.806
313	9.0	13.0	5.85	2.640	2.634	411065.9257	4737198.135
314	6.3	9.8	5.48	2.500	2.520	411067.3383	4737200.047
315	7.0	10.5	5.97	2.644	2.556	411069.1008	4737201.666
316	11.5	17.4	7.02	3.216	2.832	411071.0367	4737203.240
317	5.7	9.2	4.96	2.460	2.456	411072.8307	4737205.014
318	6.5	8.8	5.09	2.114	2.104	411076.4983	4737208.342
319	10.5	14.8	7.95	2.948	3.360	411078.2757	4737209.890
320	7.9	11.1	5.88	2.536	2.602	411081.7376	4737213.332
321	7.8	9.5	4.76	1.782	1.800	411083.6777	4737214.800
322	8.6	12.5	5.38	2.774	2.486	411085.1305	4737216.550
323	6.3	9.0	4.00	2.734	3.096	411083.5371	4737218.588
324	11.6	16.9	6.07	3.658	3.608	411082.0327	4737216.654
325	10.0	15.3	5.86	2.162	1.930	411080.1677	4737214.951
326	8.7	11.4	5.57	2.784	2.668	411078.2840	4737213.219
327	9.2	11.7	5.47	2.904	2.810	411076.5652	4737211.635
328	14.7	19.6	7.21	3.592	4.062	411074.7460	4737210.057
329	2.7	4.6	2.69	1.554	1.810	411072.8555	4737208.534
330	15.2	21.8	8.56	5.358	4.710	411071.2488	4737206.889
331	3.3	5.2	3.22	1.676	1.584	411069.4703	4737205.061
332	8.5	12.5	5.23	3.664	3.534	411067.5043	4737203.478
333	6.5	9.4	4.72	2.246	2.228	411065.7356	4737201.753
334	11.2	16.8	7.16	4.074	3.792	411064.1431	4737199.928
335	12.7	15.1	5.61	3.414	3.468	411062.2824	4737198.405
336	3.6	7.2	3.45	1.702	1.596	411065.7792	4737205.284
337	7.5	11.0	5.33	2.802	2.558	411067.7090	4737206.897
338	9.3	14.2	4.91	2.852	3.042	411069.6690	4737208.539
339	9.9	14.5	5.81	3.276	3.266	411071.3258	4737210.430
340	3.4	5.3	3.13	1.818	2.016	411073.1958	4737211.905

Tree No	Dbh (cm)	DGL (cm)	Height (m)	Crown (NS)	Crown (EW)	X Coordinate	Y Coordinate
341	9.4	12.0	6.65	2.712	2.716	411074.8106	4737213.629
342	11.0	14.2	6.17	2.716	2.412	411076.7184	4737215.049
343	6.0	8.4	4.23	2.088	2.116	411078.4303	4737216.954
344	10.2	11.6	5.82	3.138	2.648	411080.3434	4737218.472
345	6.4	9.2	5.28	1.844	1.882	411082.0476	4737220.358
346	11.2	15.4	7.00	2.970	3.054	411080.7403	4737221.665
347	12.8	17.1	6.41	3.220	3.166	411078.8100	4737220.390
348	1.6	2.8	1.94	1.102	1.056	411077.0207	4737218.552
349	10.4	15.0	5.61	3.106	3.202	411074.9764	4737217.153
350	11.0	15.3	5.72	3.270	2.872	411073.1677	4737215.289
351	11.6	16.7	5.78	3.680	3.812	411067.8483	4737210.207
352	8.7	13.1	6.23	2.562	2.594	411065.9500	4737208.628
353	9.0	14.1	5.36	3.002	3.444	411062.3379	4737205.279
354	6.0	9.2	3.86	2.408	2.248	411059.0523	4737205.341
355	1.0	2.5	1.48	0.928	0.828	411060.7161	4737207.112
356	8.2	10.9	6.08	2.528	2.686	411062.3995	4737208.818
357	10.5	14.3	5.34	2.836	2.808	411064.2214	4737210.437
358	9.6	13.4	5.29	2.602	2.450	411066.1883	4737212.084
359	9.0	12.4	5.76	2.606	2.534	411067.8622	4737213.968
360	6.0	9.5	4.51	2.002	2.042	411069.7867	4737215.354
361	8.6	11.5	5.39	2.274	2.136	411071.8013	4737216.879
362	9.2	14.0	6.10	3.039	2.852	411073.2178	4737218.812
363	8.4	12.8	5.80	2.624	2.475	411076.9431	4737222.064
364	7.5	11.0	4.12	2.222	2.192	411079.0858	4737223.425
365	0.2	1.1	0.76	0.632	0.592	411073.5145	4737222.282
366	8.3	12.6	5.78	2.954	2.472	411071.4524	4737220.446
367	9.1	11.1	6.40	2.495	2.528	411069.6384	4737218.722
368	8.9	12.8	5.87	2.456	2.412	411067.9556	4737217.193
369	9.5	13.0	6.15	3.204	3.112	411064.3881	4737213.754
370	2.1	3.4	2.58	1.176	1.070	411062.5422	4737212.104
371	10.2	13.5	6.27	3.116	2.980	411060.6580	4737210.614
372	12.6	18.2	6.40	3.484	3.455	411058.9258	4737208.828
373	6.0	9.3	3.94	1.966	1.986	411057.5626	4737207.149
374	2.0	5.0	2.06	1.160	1.110	411055.5607	4737205.372
375	10.2	14.9	6.20	3.282	2.996	411053.7268	4737207.172
376	8.8	12.9	5.23	2.845	2.995	411055.6693	4737208.862
377	1.0	3.4	1.82	1.236	1.167	411057.2204	4737210.544
378	10.1	16.3	5.40	2.976	3.026	411059.0346	4737212.418
379	8.4	12.2	6.40	2.812	2.644	411060.8836	4737213.921
380	5.6	7.8	4.43	2.138	1.990	411062.7462	4737215.484
381	6.4	10.0	5.32	2.188	2.435	411064.3319	4737217.360
382	12.4	17.9	6.63	4.004	3.924	411066.2671	4737218.873
383	9.1	13.0	6.26	3.608	3.304	411068.0054	4737220.427

Tree No	Dbh (cm)	DGL (cm)	Height (m)	Crown (NS)	Crown (EW)	X Coordinate	Y Coordinate
384	5.3	8.5	3.90	1.936	1.848	411069.7871	4737222.183
385	7.9	11.3	5.23	2.774	2.642	411073.5019	4737225.469
386	7.1	11.1	5.38	2.284	2.399	411071.8058	4737227.377
387	4.4	7.4	3.80	2.016	1.892	411070.0964	4737225.514
388	10.7	15.1	6.40	3.894	3.940	411066.2200	4737222.098
389	8.7	13.7	5.64	3.030	2.978	411064.5606	4737220.613
390	10.0	15.8	7.64	3.812	3.786	411062.6498	4737219.153
391	6.3	8.2	4.93	2.446	2.292	411060.9974	4737217.214
392	11.1	14.4	7.14	3.234	3.604	411059.1086	4737215.572
393	8.0	11.3	5.29	3.186	2.922	411055.8634	4737212.357
394	0.5	1.9	1.40	0.696	0.780	411075.0264	4737220.457
395	2.2	4.1	2.68	1.732	1.716	411054.0314	4737210.603
396	10.2	15.0	6.34	3.515	3.072	411050.3779	4737210.779
397	19.6	33.1	6.91	5.730	5.300	411052.0336	4737212.500
398	9.0	12.2	5.64	3.060	3.084	411054.1228	4737214.153
399	6.7	11.6	4.93	2.254	2.660	411055.6567	4737215.803
400	7.8	9.8	5.31	2.756	2.584	411057.5612	4737217.397
401	0.2	1.2	0.83	0.378	0.372	411059.3384	4737219.324
402	8.0	13.0	5.74	2.792	2.846	411060.9017	4737220.816
403	11.7	15.5	5.92	2.840	2.992	411062.9376	4737222.320
404	4.5	6.2	2.76	1.698	1.612	411064.6546	4737223.888
405	7.5	12.4	4.76	2.444	2.278	411066.5237	4737225.718
406	11.5	15.8	5.00	3.004	2.984	411072.2788	4737230.331
407	12.7	17.3	5.41	3.068	3.040	411070.6007	4737232.266
408	11.2	14.5	5.65	3.010	2.783	411068.5195	4737230.949
409	6.5	11.2	4.17	2.020	2.046	411061.0933	4737224.253
410	7.9	11.8	6.05	2.193	2.024	411059.2343	4737222.489
411	12.6	19.4	7.05	3.584	3.639	411057.6131	4737220.652
412	6.9	11.5	3.99	2.428	2.572	411055.7022	4737219.070
413	11.1	16.5	7.24	3.046	3.120	411053.9093	4737217.663
414	8.4	12.5	5.63	2.450	2.326	411048.6600	4737212.408
415	8.0	11.5	5.12	2.804	2.626	411045.2348	4737212.618
416	9.8	14.3	6.93	3.016	3.018	411047.0866	4737214.385
417	10.5	14.2	5.50	3.424	3.362	411049.1174	4737215.789
418	9.5	14.7	6.17	3.118	2.846	411052.1948	4737219.378
419	9.0	13.7	5.21	3.104	2.872	411054.1658	4737220.885
420	8.4	11.5	5.84	2.784	2.728	411056.2539	4737222.752
421	9.8	17.0	5.91	3.734	3.592	411057.6747	4737224.431
422	6.6	10.9	3.94	2.498	2.236	411059.4803	4737225.918
423	9.6	14.7	5.71	3.086	2.886	411063.0751	4737229.054
424	0.9	2.5	1.34	0.843	0.764	411066.6982	4737232.560
425	10.9	17.1	6.14	3.812	3.620	411068.7724	4737234.088
426	7.3	12.0	5.78	2.772	2.718	411067.0875	4737235.811

Tree No	Dbh (cm)	DGL (cm)	Height (m)	Crown (NS)	Crown (EW)	X Coordinate	Y Coordinate
427	0.0	1.9	0.91	0.690	0.663	411065.1866	4737234.412
428	8.7	13.3	5.44	2.825	2.870	411063.4633	4737232.633
429	9.3	14.6	5.86	2.652	2.714	411061.5086	4737231.052
430	5.4	8.5	4.45	1.848	1.940	411057.7810	4737227.905
431	6.4	8.9	4.83	2.136	2.048	411055.9179	4737226.125
432	7.2	10.4	6.32	2.922	2.560	411054.4341	4737224.423
433	2.0	4.4	2.59	1.280	1.252	411052.3862	4737222.694
434	5.7	9.8	4.32	2.060	1.952	411050.8833	4737221.483
435	4.0	7.1	3.65	1.986	1.684	411048.9908	4737219.520
436	10.9	16.2	6.25	3.964	3.995	411047.4354	4737217.651
437	1.4	3.2	1.82	0.992	0.998	411045.4294	4737216.121
438	7.5	11.8	4.36	2.822	2.630	411043.6011	4737214.407
439	5.5	8.2	4.48	2.070	2.076	411041.9617	4737216.148
440	12.2	19.2	5.15	4.300	3.992	411043.8103	4737218.004
441	7.8	13.0	5.85	2.724	2.676	411045.6491	4737219.469
442	12.5	17.3	6.10	3.470	3.806	411047.2917	4737221.333
443	9.8	14.9	6.48	2.943	2.832	411050.7702	4737224.629
444	0.0	1.4	1.11	0.594	0.484	411053.9404	4737227.241
445	5.5	8.5	3.36	2.390	2.144	411055.7417	4737229.386
446	9.4	13.1	6.71	3.550	3.572	411057.8551	4737231.317
447	7.0	10.2	4.90	2.308	2.094	411059.8583	4737232.873
448	7.1	12.5	5.59	2.514	2.506	411061.5237	4737234.686
449	10.1	15.3	6.47	3.024	3.040	411063.8336	4737235.647
450	6.5	11.0	4.44	2.636	2.660	411065.3973	4737237.550
451	1.6	3.9	2.01	1.298	1.202	411063.7460	4737239.519
452	5.8	10.5	4.11	2.172	2.270	411061.8594	4737237.929
453	4.4	7.9	3.66	2.114	2.130	411060.0742	4737236.222
454	7.7	13.2	5.17	2.540	2.598	411056.2572	4737233.041
455	8.1	13.8	5.05	3.506	3.190	411052.2836	4737229.470
456	0.0	1.8	0.98	0.632	0.650	411050.0259	4737228.573
457	5.5	9.4	4.38	2.092	2.008	411049.1324	4737226.330
458	7.7	10.8	5.29	2.614	2.402	411045.7287	4737223.120
459	8.8	11.5	5.47	3.060	2.996	411043.8956	4737221.312
460	0.6	3.3	1.37	0.996	0.976	411042.0838	4737219.754
461	6.1	10.5	5.08	2.500	2.360	411040.3164	4737218.039
462	3.8	7.3	3.10	1.814	2.200	411038.6756	4737219.748
463	12.2	18.4	5.78	4.220	3.994	411040.3849	4737221.506
464	5.8	9.8	4.38	2.536	2.380	411042.3897	4737223.056
465	7.5	11.8	5.36	2.476	2.474	411043.9548	4737224.855
466	2.9	4.6	3.04	1.486	1.458	411045.5715	4737226.614
467	11.2	16.4	6.77	4.150	3.436	411047.4895	4737228.223
468	4.8	7.7	3.95	1.678	1.782	411049.4521	4737229.706
469	14.2	19.8	7.29	4.058	3.944	411051.0998	4737231.619

Tree No	Dbh (cm)	DGL (cm)	Height (m)	Crown (NS)	Crown (EW)	X Coordinate	Y Coordinate
470	6.2	8.1	4.80	2.196	2.120	411054.5448	4737234.842
471	6.1	8.4	4.90	2.352	2.560	411056.5696	4737236.520
472	5.9	10.5	4.68	2.194	2.296	411058.4686	4737238.041
473	7.7	13.0	3.90	2.796	2.528	411062.2740	4737241.142
474	3.0	6.3	2.81	1.776	1.674	411060.5831	4737242.957
475	5.5	8.1	4.90	2.358	2.522	411054.9139	4737238.286
476	5.8	9.4	4.28	2.532	2.208	411052.7949	4737236.651
477	5.3	8.3	3.92	2.154	2.048	411051.1045	4737234.948
478	7.7	11.9	7.14	2.442	2.356	411047.8326	4737231.488
479	11.0	15.5	5.72	3.440	3.200	411044.1905	4737228.144
480	5.4	8.6	3.60	2.010	2.026	411042.4712	4737226.415
481	7.0	10.2	5.58	2.716	2.732	411040.7123	4737224.802
482	10.8	17.7	5.60	3.638	3.722	411037.0040	4737221.503
483	5.5	9.3	4.75	2.242	2.380	411035.3463	4737223.295
484	10.4	15.5	6.64	3.950	3.402	411037.0723	4737225.020
485	8.9	14.1	5.82	3.094	3.136	411039.0317	4737226.609
486	8.6	15.5	6.03	3.868	3.548	411040.6629	4737228.412
487	7.0	9.8	4.36	2.516	2.472	411042.3042	4737230.184
488	9.6	15.5	6.57	3.236	3.006	411044.1708	4737231.687
489	1.2	2.2	1.79	1.038	0.987	411046.2235	4737233.268
490	7.7	11.7	5.85	2.604	2.316	411049.5000	4737236.663
491	4.4	7.8	3.74	2.314	2.182	411051.0839	4737238.475
492	9.5	14.3	6.75	2.774	2.766	411053.2009	4737240.063
493	1.4	2.4	1.62	1.012	0.988	411056.7729	4737243.427
494	8.4	11.6	6.86	3.056	3.120	411055.1816	4737244.931
495	6.0	11.2	3.66	2.682	2.668	411051.5423	4737241.817
496	9.4	14.0	5.45	3.156	3.192	411049.5338	4737240.177
497	8.4	12.7	6.08	2.362	2.372	411047.8508	4737238.461
498	6.4	10.8	4.35	2.770	2.462	411045.8330	4737236.863
499	9.2	13.8	5.91	3.006	3.052	411044.3470	4737235.177
500	7.3	11.1	5.82	2.472	2.320	411042.1066	4737233.678
501	10.2	16.7	5.73	3.454	3.452	411040.5927	4737231.823
502	9.0	14.4	6.44	2.658	2.368	411038.9793	4737230.073
503	10.2	14.8	6.11	3.472	3.394	411037.3663	4737228.511
504	10.6	13.8	5.96	3.518	3.214	411035.3340	4737226.805
505	8.0	13.4	5.63	3.106	3.240	411033.6061	4737225.124
506	1.5	3.5	1.94	1.400	1.278	411031.9152	4737226.801
507	2.8	4.8	3.04	1.416	1.504	411033.7835	4737228.444
508	6.5	10.1	4.50	2.548	2.382	411035.7442	4737230.212
509	3.9	6.9	3.29	1.732	1.532	411037.3043	4737231.821
510	9.9	13.9	6.44	2.962	2.924	411039.0033	4737233.544
511	1.0	2.4	1.57	0.988	0.946	411040.4984	4737235.554
512	11.8	17.2	7.16	2.874	2.944	411042.6478	4737236.884

Tree No	Dbh (cm)	DGL (cm)	Height (m)	Crown (NS)	Crown (EW)	X Coordinate	Y Coordinate
513	6.1	8.5	4.77	2.518	2.346	411044.5332	4737238.682
514	8.9	13.3	4.36	3.374	3.114	411046.1197	4737240.263
515	6.2	10.2	4.49	2.252	2.308	411049.9250	4737243.446
516	0.7	2.8	1.59	1.024	0.920	411055.2972	4737248.242
517	8.0	15.1	5.32	2.678	2.412	411049.9580	4737246.710
518	9.4	12.6	5.38	2.682	2.782	411048.1385	4737245.345
519	3.3	6.7	3.08	1.470	1.662	411046.5557	4737243.454
520	6.4	9.5	3.65	2.458	2.314	411044.5803	4737241.937
521	3.4	6.7	3.39	1.722	1.800	411042.6221	4737240.220
522	8.6	11.7	5.66	2.760	2.760	411040.8939	4737238.701
523	10.0	14.8	6.10	2.912	2.838	411038.9776	4737237.010
524	1.7	3.4	2.10	1.164	1.128	411037.1665	4737235.321
525	4.9	7.9	4.38	2.004	2.006	411035.7076	4737233.667
526	11.6	18.4	5.97	3.524	3.408	411034.0456	4737231.975
527	3.5	6.6	3.08	1.508	1.608	411031.9904	4737230.240
528	1.5	3.4	1.93	1.076	1.700	411030.2232	4737228.553
529	4.2	7.5	3.97	1.888	1.822	411028.5831	4737230.372
530	4.9	8.7	4.48	2.158	2.346	411032.3312	4737233.729
531	7.2	10.0	4.84	2.636	2.332	411034.0284	4737235.446
532	11.2	15.5	8.10	3.582	3.726	411035.4537	4737237.143
533	5.5	9.7	4.90	2.232	2.066	411037.2681	4737238.700
534	6.5	10.4	3.61	2.508	2.416	411039.2244	4737240.373
535	4.5	7.5	3.68	1.864	2.076	411040.6189	4737242.040
536	7.6	12.1	4.82	3.022	3.130	411042.9510	4737243.834
537	10.5	14.3	6.15	2.806	3.094	411044.7096	4737245.457
538	12.8	17.4	7.64	3.436	3.386	411046.4913	4737247.112
539	8.5	11.7	5.56	2.354	2.482	411048.3733	4737248.585
540	9.3	15.1	5.14	2.688	2.848	411050.1318	4737250.330
541	8.4	12.5	4.82	3.070	2.732	411052.1668	4737251.791
542	8.9	13.3	6.09	2.624	2.474	411048.5621	4737252.148
543	7.2	11.6	5.19	2.896	2.742	411046.8801	4737250.525
544	11.4	16.3	6.64	3.394	3.082	411044.8603	4737248.946
545	6.2	9.3	5.32	2.378	2.168	411042.9275	4737247.147
546	10.7	15.8	7.05	3.242	3.296	411041.2548	4737245.522
547	7.1	12.3	4.06	2.746	2.680	411037.5526	4737242.286
548	9.8	14.3	7.16	3.406	3.644	411035.7559	4737240.590
549	5.2	9.7	4.26	2.416	2.318	411033.8041	4737239.008
550	9.6	1.4	6.70	2.566	2.710	411032.1826	4737237.251
551	4.2	8.3	4.14	2.306	2.214	411030.6788	4737235.440
552	2.9	6.0	2.98	1.356	1.512	411028.9245	4737233.532
553	9.4	15.2	6.56	3.288	3.374	411026.8711	4737232.093
554	7.1	12.6	3.80	2.294	2.732	411025.1248	4737233.811
555	11.3	17.4	6.96	4.318	3.948	411030.4981	4737239.068

Tree No	Dbh (cm)	DGL (cm)	Height (m)	Crown (NS)	Crown (EW)	X Coordinate	Y Coordinate
556	3.0	5.3	2.50	1.632	1.614	411032.2518	4737241.025
557	3.0	5.0	2.84	1.543	1.634	411034.0360	4737242.533
558	10.3	15.4	5.88	2.954	2.932	411036.2094	4737243.938
559	10.1	14.8	6.40	3.002	2.578	411037.4285	4737245.840
560	2.9	4.7	3.04	1.596	1.478	411039.3803	4737247.272
561	8.5	13.4	5.00	3.130	2.926	411041.2696	4737248.897
562	9.8	14.7	6.17	3.339	3.166	411043.0537	4737250.607
563	12.9	18.5	7.79	4.124	3.802	411045.2367	4737252.402
564	5.0	8.8	3.97	1.756	1.640	411049.0699	4737255.386
565	9.1	13.7	5.87	3.076	3.062	411045.9522	4737258.956
566	8.8	11.8	6.09	2.602	2.508	411045.4049	4737255.919
567	9.6	13.8	6.17	3.018	2.888	411043.6653	4737254.196
568	8.0	11.2	6.07	2.674	2.738	411041.7597	4737252.718
569	8.5	13.4	6.13	2.924	2.560	411039.8212	4737251.179
570	9.6	15.1	5.93	3.394	3.588	411037.8141	4737249.038
571	0.6	2.0	1.47	1.052	0.954	411035.6434	4737247.726
572	8.5	11.7	5.95	2.816	2.890	411034.1779	4737245.824
573	11.9	18.8	6.81	3.746	4.036	411032.2387	4737244.104
574	4.9	7.9	4.44	2.070	1.992	411030.7622	4737242.927
575	7.6	12.4	5.23	2.862	2.934	411028.9899	4737241.214
576	7.6	11.0	5.22	3.162	2.522	411027.3919	4737238.788
577	8.7	14.0	4.96	2.694	2.782	411025.3506	4737237.448
578	5.5	8.8	3.82	2.662	2.588	411021.9741	4737237.458
579	10.4	15.0	7.02	3.420	3.426	411023.6031	4737239.254
580	4.7	6.7	4.48	2.278	1.962	411025.6027	4737240.761
581	3.8	6.8	3.40	1.852	1.958	411027.2381	4737242.528
582	4.1	6.6	3.87	2.142	1.926	411028.7968	4737244.332
583	8.8	11.8	5.36	2.928	2.392	411030.6603	4737245.913
584	5.8	8.4	5.47	2.430	2.312	411032.6832	4737247.355
585	12.0	17.9	6.67	3.996	4.088	411034.0518	4737249.424
586	6.8	9.0	5.06	2.152	2.272	411036.2251	4737250.630
587	7.8	11.7	5.56	3.056	2.762	411037.8754	4737252.297
588	8.4	12.3	5.64	2.584	2.568	411039.9847	4737254.545
589	6.0	8.5	4.64	2.246	2.156	411041.9875	4737256.074
590	3.6	6.4	3.15	1.794	1.970	411042.2890	4737259.705
591	12.9	18.1	7.42	3.514	3.406	411040.4607	4737257.937
592	7.4	10.4	3.96	2.716	2.804	411038.4457	4737256.475
593	11.0	15.3	6.07	3.222	3.194	411036.7442	4737254.855
594	9.0	12.6	5.57	2.897	2.922	411034.8382	4737253.298
595	10.5	13.7	5.92	2.834	2.828	411032.6217	4737250.851
596	10.8	17.0	4.67	3.936	4.354	411030.7749	4737249.182
597	4.4	7.6	4.26	2.512	2.268	411027.1778	4737246.233
598	6.2	10.4	4.56	2.562	2.666	411025.5870	4737244.440

Tree No	Dbh (cm)	DGL (cm)	Height (m)	Crown (NS)	Crown (EW)	X Coordinate	Y Coordinate
599	4.3	8.0	3.34	1.876	1.822	411023.9761	4737242.612
600	4.4	8.2	3.97	2.050	2.140	411021.9988	4737241.095
601	7.7	11.5	5.23	2.586	2.414	411018.5308	4737241.032
602	7.7	12.2	5.79	2.362	2.196	411020.4057	4737242.853
603	7.3	10.9	5.09	2.270	2.574	411022.2857	4737244.554
604	3.2	5.0	3.05	1.766	2.104	411023.9154	4737246.118
605	4.1	6.7	4.28	2.032	2.418	411025.4109	4737247.955
606	7.5	12.7	4.81	2.624	2.336	411027.3161	4737249.826
607	9.8	15.0	4.62	2.972	3.388	411031.1697	4737252.863
608	10.6	15.3	4.97	3.524	3.308	411032.7113	4737254.198
609	9.4	11.7	5.97	3.012	3.186	411035.0998	4737256.772
610	8.3	11.7	5.64	2.906	3.068	411037.0157	4737258.234
611	4.5	6.7	3.97	1.874	2.018	411038.8225	4737259.661
612	7.8	11.7	5.98	3.436	3.484	411040.5141	4737261.631
613	0.0	1.6	1.01	0.458	0.562	411043.8186	4737257.683
614	8.3	15.0	4.33	2.882	3.150	411041.1187	4737264.523
615	3.4	5.0	3.54	1.618	1.442	411039.1073	4737263.395
616	3.9	6.5	3.81	1.628	1.726	411037.2744	4737261.696
617	10.5	18.3	5.90	3.688	3.574	411035.4521	4737260.106
618	2.5	4.1	3.14	1.462	1.426	411033.8873	4737258.412
619	7.5	10.9	4.13	2.758	2.952	411031.7648	4737256.912
620	5.5	8.2	5.11	2.226	2.492	411029.6107	4737255.762
621	8.0	12.8	4.61	2.260	2.850	411025.6910	4737251.714
622	4.6	7.7	3.69	1.966	2.404	411023.8587	4737249.843
623	2.0	4.1	2.17	1.384	1.158	411022.1877	4737248.066
624	5.4	8.5	4.71	2.308	2.082	411020.8246	4737246.288
625	3.2	5.4	3.22	1.798	2.868	411018.9495	4737244.518
626	9.1	12.7	5.06	3.074	3.178	411016.9667	4737242.890
627	9.3	13.7	6.27	3.068	3.316	411015.3775	4737244.673
628	9.8	6.4	5.22	1.836	1.842	411017.0392	4737246.641
629	7.2	10.9	4.53	2.678	2.746	411018.8499	4737248.201
630	6.3	10.3	4.97	3.024	2.746	411020.8349	4737249.771
631	1.9	3.0	1.92	1.106	1.156	411022.4755	4737251.631
632	8.3	11.2	5.78	2.556	3.012	411024.1192	4737253.402
633	7.9	11.4	6.02	2.394	2.558	411026.0698	4737254.702
634	4.9	8.4	4.50	2.024	2.166	411027.9606	4737257.596
635	8.9	13.1	5.43	2.722	2.754	411030.1542	4737258.919
636	5.4	8.2	3.90	2.024	2.064	411033.8864	4737261.854
637	8.5	11.0	6.32	3.692	3.322	411037.2914	4737265.299
638	0.0	1.1	0.69	0.558	0.438	411039.1818	4737266.752
639	4.1	7.4	2.88	1.874	1.946	411035.6988	4737266.959
640	3.2	6.1	3.27	1.912	1.596	411033.9027	4737265.610
641	10.7	14.1	6.23	2.714	3.116	411032.3685	4737263.827

Tree No	Dbh (cm)	DGL (cm)	Height (m)	Crown (NS)	Crown (EW)	X Coordinate	Y Coordinate
642	6.1	9.5	4.15	2.244	2.162	411030.0970	4737262.300
643	10.8	15.6	6.75	3.424	3.122	411028.5990	4737260.768
644	4.5	7.5	3.49	2.940	2.864	411026.3842	4737259.469
645	0.0	1.5	1.20	0.672	0.660	411024.7361	4737257.800
646	5.5	8.9	4.76	2.342	2.514	411019.1739	4737251.777
647	7.9	13.3	3.55	3.074	3.224	411015.7306	4737248.613
648	4.5	7.4	4.07	1.934	1.730	411012.1843	4737248.467
649	5.0	8.1	3.76	2.572	2.466	411015.9231	4737252.020
650	4.2	6.3	3.69	1.836	1.612	411017.6085	4737253.503
651	1.6	3.2	1.83	1.034	1.066	411018.9929	4737255.393
652	7.4	11.0	5.29	2.606	2.830	411020.6735	4737256.999
653	3.4	5.0	3.71	2.056	2.974	411022.8577	4737258.198
654	7.4	11.3	5.69	2.564	2.878	411024.0615	4737260.201
655	2.0	3.9	2.01	1.298	1.132	411026.9880	4737262.592
656	0.0	1.6	0.94	0.802	0.744	411028.8077	4737264.128
657	4.1	6.7	3.59	2.192	1.816	411030.7508	4737265.677
658	10.8	14.8	6.39	2.630	3.256	411032.4122	4737267.209
659	11.3	16.1	5.55	3.822	3.442	411034.0206	4737268.724
660	5.9	8.5	4.32	2.194	1.932	411036.0892	4737270.065
661	1.7	3.2	2.00	1.294	1.352	411032.4807	4737270.794
662	2.2	3.5	2.37	0.864	1.652	411029.1457	4737267.500
663	4.5	7.6	4.15	1.914	1.652	411025.3675	4737264.510
664	7.4	11.7	5.13	2.802	2.762	411022.2471	4737261.732
665	3.7	6.8	3.20	1.540	1.458	411020.9592	4737259.838
666	7.7	11.6	4.68	2.434	2.636	411019.1693	4737258.108
667	0.0	1.8	1.03	0.562	0.620	411017.4226	4737257.115
668	12.9	19.9	6.41	4.032	3.856	411015.9159	4737255.395
669	4.1	7.4	3.54	1.948	1.984	411014.3051	4737253.816
670	5.2	9.4	4.58	2.142	2.232	411010.7073	4737250.436
671	6.5	10.4	4.31	2.326	2.380	411010.9103	4737254.045
672	6.9	11.6	5.45	3.318	2.998	411012.5823	4737255.509
673	7.3	10.3	4.52	2.764	2.548	411014.2411	4737257.219
674	2.6	5.1	2.25	1.648	1.742	411015.5514	4737259.101
675	2.0	5.0	2.23	1.270	1.292	411019.0205	4737261.284
676	4.6	9.3	3.96	2.236	2.126	411022.2908	4737264.819
677	5.0	7.4	4.08	2.032	2.086	411025.7878	4737268.059
678	9.3	13.8	6.12	3.084	2.852	411027.5410	4737269.501
679	8.4	13.3	5.97	2.778	2.900	411030.9540	4737272.604
680	8.5	11.9	4.76	3.054	2.714	411032.9443	4737273.819
681	7.5	11.9	4.40	2.810	3.042	411031.3136	4737275.635
682	3.7	6.6	3.61	1.650	1.816	411029.2131	4737274.526
683	9.3	14.4	6.61	2.914	2.662	411026.0185	4737271.356
684	8.6	13.6	5.78	2.878	2.950	411024.1305	4737269.800

Tree No	Dbh (cm)	DGL (cm)	Height (m)	Crown (NS)	Crown (EW)	X Coordinate	Y Coordinate
685	3.2	6.0	2.88	1.602	1.610	411022.2625	4737268.269
686	5.2	8.6	3.82	1.834	1.734	411017.2868	4737263.043
687	7.4	11.6	4.89	2.996	2.924	411020.8637	4737270.138
688	2.6	4.2	2.76	1.336	1.120	411024.2703	4737273.234
689	11.7	17.0	5.95	4.074	3.306	411026.0862	4737274.621
690	8.5	16.3	4.60	3.058	2.938	411029.7794	4737277.498
691	1.5	2.6	2.02	1.116	1.154	411122.1758	4737177.269
692	0.0	1.4	0.65	0.356	0.364	411086.5862	4737200.871
693	0.9	2.7	1.35	0.716	1.082	411064.0131	4737203.442
694	0.0	0.9	0.46	0.230	0.344	411052.1229	4737216.135
695	0.0	1.1	0.69	0.428	0.538	411058.1360	4737234.647
696	0.0	1.2	0.79	0.366	0.440	411052.6904	4737233.545

Curriculum Vitae

EDUCATION

2019 **MASTER OF SCIENCE IN FORESTRY**

SUNY College of Environmental Sciences and Forestry, Syracuse, NY.

Master's Degree Candidate, Graduate Program in Environmental Science

Graduate Advisor: Dr. Eddie Bevilacqua

Thesis Title: "Evaluation of UAS imagery for forest regeneration surveys"

2013 **BACHELOR'S DEGREE IN FORESTRY**

(Honor Degree)

Karadeniz Technical University, Trabzon, Turkey

Department of Forest Engineer

PROFESSIONAL EXPERIENCE

2014 Work as a Forest Engineer, Erkar Forestry

Kutahya, Turkey

Forest monitoring and surveys. The work required technical skills such as in GPS, cartography, and tree ID.

2013 Work as a Forest Engineer, Erkar Forestry

Antep, Maras, and Hatay, Turkey

Forest monitoring and surveys. The work required technical skills such as in GPS, cartography, and tree ID.

2012 Internship as Forest Engineer at 31st chief engineer management

Gumushane, Turkey

Application of basic knowledge and skills in forestry

2011 Internship on mapping via ArcGIS at Laboratory of Forest Management at the Karadeniz Technical University

Trabzon, Turkey

Creating data set and creating maps in ArcGIS

SUCCESS AND SCHOLARSHIPS

2019 Winner of "**The Best Poster award at STRATUS 201**9" (Systems and Technologies for Remote Sensing Applications Through Unmanned Aerial Systems), Rochester, NY.

2014 Turkish Ministry of Education Full Non-Return Scholarship to complete a master's degree.

2013 Honor Degree obtained when graduating from Karadeniz Technical University

POSTER PRESENTATIONS

April 16, 2019	2019 Spotlight on Student Research Symposium Syracuse, New York.
February 27, 2019	STRATUS 2019 Rochester, NY. 25-27 February 2019.
January 24, 2019	NYSAF 2019 Annual Meeting Syracuse, New York. January 23-25, 2019.

LICENSES

Remote Pilot, Certificate Number: 4142821, 11 Jun 2018

COMPUTER & TECHNICAL SKILLS

Expert	ArcGIS for Desktop, Word and Excel Microsoft Office Extensions
Proficient	SPSS, Minitab, Trimble Tripod GPS, Mission Planner, GeoSetter, Python.

Beginner R, Pix4d, Agisoft Metashape

VOLUNTEERING EXPERIENCE

Fall 2018 Volunteered as a Teaching Assistant in the course ESF 300: Introduction to Geospatial Information Technologies at SUNY ESF. My role was to assist students during their lab hours.

2018-2019 Food Recovery Network at Syracuse University and SUNY ESF,
This organization help to distribute donated dining hall food to local charitable organizations to reduce food waste.